A generative AI-discovered TNIK inhibitor for idiopathic pulmonary fibrosis: a randomized phase 2a trial

A list of authors and their affiliations appears at the end of the paper

Despite substantial progress in artificial intelligence (AI) for generative chemistry, few novel AI-discovered or AI-designed drugs have reached human clinical trials. Here we present the results of the first phase 2a multicenter, double-blind, randomized, placebo-controlled trial testing the safety and efficacy of rentosertib (formerly ISM001-055), a first-in-class AI-generated small-molecule inhibitor of TNIK, a first-in-class target in idiopathic pulmonary fibrosis (IPF) discovered using generative AI. IPF is an age-related progressive lung condition with no current therapies available that reverse the degenerative course of disease. Patients were randomized to 12 weeks of treatment with 30 mg rentosertib once daily (QD, $n = 18$), 30 mg rentosertib twice daily (BID, $n = 18$), 60 mg rentosertib QD ($n = 18$) or placebo ($n = 17$). The primary endpoint was the percentage of patients who have at least one treatment-emergent adverse event, which was similar across all treatment arms (72.2% in patients receiving 30 mg rentosertib QD ($n = 13/18$), 83.3% for 30 mg rentosertib BID ($n = 15/18$), 83.3% for 60 mg rentosertib QD ($n = 15/18$) and 70.6% for placebo ($n = 12/17$)). Treatment-related serious adverse event rates were low and comparable across treatment groups, with the most common events leading to treatment discontinuation related to liver toxicity or diarrhea. Secondary endpoints included pharmacokinetic dynamics (C_{max}, C_{trough}, t_{max}, $AUC_{0-t/\tau/\infty}$ and $t_{1/2}$), changes in lung function as measured by forced vital capacity, diffusion capacity of the lung for carbon monoxide, forced expiry in 1 s and change in the Leicester Cough Questionnaire score, change in 6-min walk distance and the number and hospitalization duration of acute exacerbations of IPF. We observed increased forced vital capacity at the highest dosage with a mean change of +98.4 ml (95% confidence interval 10.9 to 185.9) for patients in the 60 mg rentosertib QD group, compared with −20.3 ml (95% confidence interval −116.1 to 75.6) for the placebo group. These results suggest that targeting TNIK with rentosertib is safe and well tolerated and warrants further investigation in larger-scale clinical trials of longer duration. ClinicalTrials.gov registration number: NCT05938920.

✉e-mail: xuzj@hotmail.com; alex@insilico.com

The process of developing novel therapeutics is increasingly slow and costly[1], with an average of US$2–3 billion spent over the course of 10–15 years to bring a new drug to market[2]. Advances in artificial intelligence (AI) have demonstrated proof-of-concept innovation and potential to accelerate and decrease costs across all stages of pharmaceutical research and development by facilitating disease-associated target prioritization[3–5], compound design and optimization[6–10], and clinical trial performance[11–15]. Shifting more of the time-, material- and labor-intensive steps of drug discovery to AI platforms enables more rapid nomination of therapeutic candidate compounds that explore the possible chemical space more thoroughly[16,17] and with a concomitant reduction in hands-on screening[18,19], thus allowing more preclinical candidate compounds to enter clinical testing and, eventually, clinical practice.

Despite these advancements, few AI-discovered or AI-designed drugs have reached clinical trials. AI-discovered drugs have experienced similar levels of phase 2 trial failure as non-AI-discovered drugs[20,21], and none has so far progressed through phase 3 trials[21]. The question of whether AI can impart meaningful, sustained disruption to drug development has remained unanswered[21].

As an answer to this question, our group used generative AI-driven discovery tools[22,23] to identify Traf2- and Nck-interacting kinase (TNIK) de novo as a critical regulator of idiopathic pulmonary fibrosis (IPF) pathology as it orchestrates multiple profibrotic and proinflammatory cellular programs[9]. Our approach resulted in the first antifibrotic, small-molecule TNIK inhibitor, rentosertib (formerly ISM001-055), for the treatment of IPF designed by generative AI. We reported the development and positive phase 0 and 1 trial results of rentosertib[9] (NCT05154240 and CTR20221542 (accessed via http://www.chinadrugtrials.org.cn/)), the first report of a targeted TNIK inhibitor entering clinical testing, which found rentosertib to be safe and well tolerated by healthy individuals, exhibiting a favorable pharmacokinetic (PK) profile in both trials[9]. This was also, importantly, the first reported instance of AI platform-enabled discovery of both a disease-associated target and a compound for that target. Our generative AI-powered approach streamlined preclinical candidate nomination to a mere 18 months and completion of phase 0/1 clinical testing to under 30 months from the initiation of target discovery, representing a revolutionary shift in the streamlining of drug discovery[9].

IPF is an age-related, progressive lung disease diagnosed by excluding other potential causes of interstitial lung disease (for example, environmental exposures, connective tissue disease, hypersensitivity pneumonitis or drug toxicities)[24] and marked by interstitial pneumonia, dyspnea and cough[25], histologically characterized by fibroblast proliferation and extracellular matrix remodeling[26–29]. Affecting between 10 and 60 per 100,000 individuals in the USA, with an approximately tenfold greater incidence in those over 65, IPF occurs at a rate similar to stomach, brain and testicular cancers[25]. The median survival time after diagnosis is 2–4 years despite widespread availability of targeted antifibrotic therapies[26,30], highlighting the ongoing need for novel, effective therapies to treat IPF. The current standard-of-care (SOC) therapy regimen to treat IPF includes either nintedanib, a broadly acting inhibitor of receptor tyrosine kinases[31], or pirfenidone, an inhibitor of TGFβ-mediated fibroblast-to-myofibroblast transition[32]. Clinical trials investigating these two drugs in patients with IPF have demonstrated only a slowing of disease progression[33,34], as measured by forced vital capacity (FVC) and self-reported quality of life (QOL) metrics, and unclear benefit to survival[26], making the development of therapies that can restore lung function and reverse the course of disease a priority.

Here, we present the results of a phase 2a multicenter, double-blind, randomized, placebo-controlled trial to assess the safety, tolerability, PK and impact on FVC of rentosertib at a range of doses for up to 12 weeks in patients with IPF. Additional secondary and exploratory endpoints and analyses were designed to further measure lung function, QOL metrics and cellular phenotypes associated with rentosertib treatment and response.
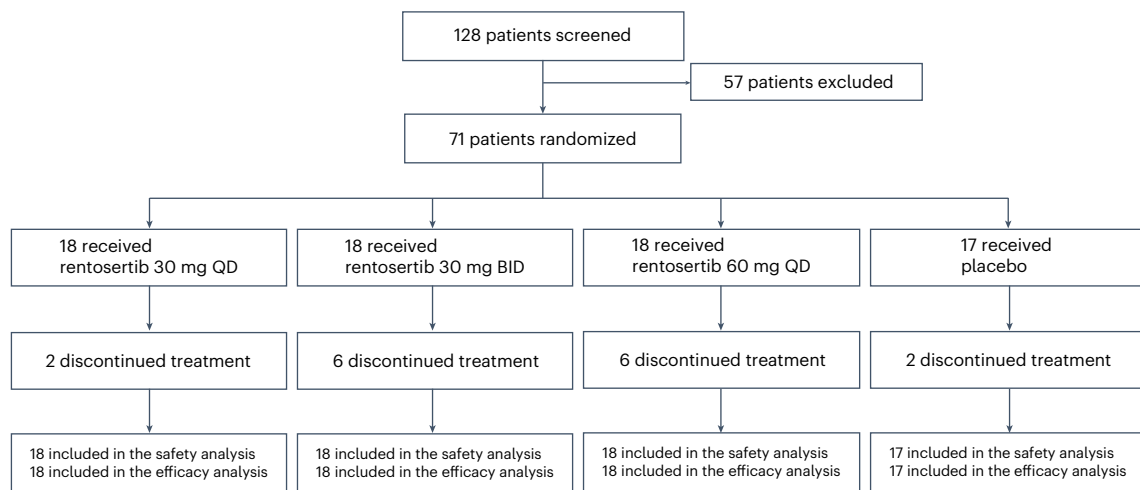
Results

Patients

Among the 128 patients screened for inclusion, 71 (55.5%) patients were enrolled and randomly assigned to receive placebo ($n = 17$), 30 mg rentosertib once daily (QD, $n = 18$), 30 mg rentosertib twice daily (BID, $n = 18$) or 60 mg rentosertib QD ($n = 18$) (Extended Data Fig. 1). The most common reason for screening-based exclusion was obstructive pulmonary disease comorbidity indicated by forced expiry in 1 s (FEV1)/FVC less than 0.7 at visit 1 (baseline) or diffusion capacity of the lung for carbon monoxide (DLCO) percent of predicted normal falling outside the range of ≥25% and <80% at baseline. Patients were also excluded for a recent history of upper or lower respiratory tract infection (within 4 weeks) at visit 1 (baseline) or before visit 2 (week 1). The intention-to-treat population included 71 patients, and 55 (77%) completed the 12-week placebo-controlled period (15 (88%) in the placebo group, 16 (89%) in the 30 mg rentosertib QD group, 12 (67%) in the 30 mg rentosertib BID group and 12 (67%) in the 60 mg rentosertib QD group). Overall, 16 (22.5%) patients discontinued treatment before the conclusion of the 12-week study due to either adverse events (AEs) or other withdrawal; 2 from placebo, 2 from 30 mg rentosertib QD, 6 from 30 mg rentosertib BID and 6 from 60 mg rentosertib QD groups. All patients were included in the safety and efficacy analyses (Fig. 1).

Clinical and demographic characteristics, including age, body mass index (BMI) and baseline lung function, were similar across treatment groups (Table 1).

Primary safety endpoint

The rates of treatment-emergent AEs (TEAEs) were similar across all treatment groups (13/18 (72.2%) in the 30 mg rentosertib QD group, 15/18 (83.3%) in the 30 mg rentosertib BID group, 15/18 (83.3%) in the 60 mg rentosertib QD group and 12/17 (70.6%) in the placebo group) (Table 2), with similar incidence for patients concurrently taking SOC antifibrotic therapy or not (Supplementary Table 1). Treatment-related AEs were more common among patients who received rentosertib compared with placebo, with 5/17 (29.4%) in the placebo group versus 9/18 (50.0%) in the 30 mg QD group, 11/18 (61.1%) in the 30 mg BID group, and 14/18 (77.8%) in the 60 mg QD group. Of these, few were serious AEs (SAEs), with no treatment-related SAEs reported in the placebo group, 1/18 (5.6%) of the rentosertib 30 mg QD group, 2/18 (11.1%) in the 30 mg BID group and 2/18 (11.1%) in the 60 mg QD group (Table 2). The most common TEAEs were hypokalemia (2 in placebo (11.8%), 3 in 30 mg QD (16.7%), 5 in 30 mg BID (27.8%) and 3 in 60 mg QD (20.4%)), hepatic function abnormal (2 in placebo (11.8%), 2 in 30 mg QD (11.1%), 4 in 30 mg BID (22.2%), diarrhea (0 in placebo, 2 in 30 mg QD (11.1%), 3 in 30 mg BID (16.7%) and 5 in 60 mg QD (27.8%)) and alanine aminotransferase (ALT) increase (1 in placebo (5.9%), 1 in 30 mg QD (5.6%), 1 in 30 mg BID (5.6%), 6 in 60 mg QD (33.3%) and 3 in 60 mg QD (16.7%)). A complete listing of TEAEs is presented in Supplementary Table 2.

The most frequent reason for treatment discontinuation was AEs (12/16 (75%)), and the treatment of 7 of the 12 patients was discontinued for AEs due to liver injury or dysfunction (0/18 (0%) in the 30 mg QD group, 4/18 (22.2%) in the 30 mg BID group and 3/18 (17%) in the 60 mg QD group) (Supplementary Table 3). Four of the seven (57.1%) total participants who withdrew because of liver toxicity were concurrently administered nintedanib antifibrotic therapy. Three of the four (75%) remaining discontinuations were due to patient withdrawal from the trial (3/71 patients (4.2%)). One patient died of heart failure before the week 12 end-of-treatment (EOT) visit determined to be unrelated to the trial owing to a history of degenerative aortic valve disease, aortic valve incompetence, left ventricular dysfunction, aortic dilatation, pulmonary hypertension, increased blood glucose and hypercholesterolemia, as well as a lack of other AEs reported and no notable findings for vital signs, physical examination, 12-lead electrocardiogram (ECG) or laboratory tests since randomization. A complete listing of patients whose treatment was discontinued due to TEAE is presented in Supplementary Table 4.

```
                              ┌──────────────────────────┐
                              │   128 patients screened  │
                              └──────────────────────────┘
                                          │
                                          │          ┌──────────────────────────┐
                                          ├─────────▶│   57 patients excluded   │
                                          │          └──────────────────────────┘
                              ┌──────────────────────────┐
                              │   71 patients randomized │
                              └──────────────────────────┘
```

18 received rentosertib 30 mg QD	18 received rentosertib 30 mg BID	18 received rentosertib 60 mg QD	17 received placebo
2 discontinued treatment	6 discontinued treatment	6 discontinued treatment	2 discontinued treatment
18 included in the safety analysis 18 included in the efficacy analysis	18 included in the safety analysis 18 included in the efficacy analysis	18 included in the safety analysis 18 included in the efficacy analysis	17 included in the safety analysis 17 included in the efficacy analysis

Fig. 1 | Trial participant randomization and follow-up scheme. Of 128 patients screened for inclusion, 71 were randomized to receive 30 mg rentosertib QD (n = 18), 30 mg rentosertib BID (n = 18), 60 mg rentosertib QD (n = 18), or placebo (n = 17) over the course of 12 weeks. Sixteen patients discontinued treatment prior to the end of treatment.

Secondary lung function endpoints

FVC is the gold-standard metric for assessing the lung function of patients with IPF and response to therapeutic intervention[33–35]. After 12 weeks of treatment, patients who received placebo experienced deteriorating FVC with a mean change of −20.3 ml (95% confidence interval (CI) −116.1 to 75.6). Patients who received 30 mg rentosertib QD showed a similar mean reduction in FVC of −27.0 ml (95% CI −88.8 to 34.8), patients who received 30 mg rentosertib BID experienced a mean change of +19.7 ml (95% CI −60.5 to 99.9) and patients receiving 60 mg rentosertib QD showed improved FVC, with and +98.4 ml (95% CI 10.9 to 185.9) (Fig. 2 and Extended Data Fig. 2). Patients receiving 60 mg rentosertib QD not concurrently taking SOC antifibrotic therapy exhibited significant improvement in FVC (+187.8 ml, 95% CI 68.6 to 306.9 ml), whereas patients concurrently taking 60 mg rentosertib QD with either nintedanib or pirfenidone did not exhibit significant changes in FVC (Extended Data Fig. 3).

The changes in DLCO and FEV1 were relatively small and similar across treatment regimens (Extended Data Fig. 4a–e). Changes in self-reported QOL and physical ability metrics, such as responses to the Leicester Cough Questionnaire (LCQ) and 6-min walk distance (6MWD), respectively, were likewise similar across treatment groups (Extended Data Fig. 4f–i), although our modeling indicated a significant increase of least-squares mean change of the LCQ scores of patients receiving 60 mg rentosertib compared with those receiving placebo (two-sided P = 0.0495).

Three patients (16.7%) receiving 60 mg rentosertib QD and one patient (5.9%) receiving placebo experienced acute exacerbation of IPF (AE-IPF) (Supplementary Table 5). The patients in the 60 mg QD group were all hospitalized in response to their acute exacerbations with a mean duration of 23.3 days, whereas the patient in the placebo group was not hospitalized.

Post-hoc exploratory analyses

Pharmacokinetics. A PK analysis of rentosertib concentration in the blood plasma of patients with IPF after single and multiple doses shows a favorable PK profile, with greater exposure in patients receiving 60 mg rentosertib QD compared with patients receiving 30 mg rentosertib QD or 30 mg rentosertib BID, peaking 1 h after administration (Fig. 3a–c and Supplementary Table 6). The area under the plasma–concentration curve (AUC_{0-t}), measuring total exposure to the drug to the last available time point, was greater for the 60 mg rentosertib QD at both week 0 (first dose) and week 12 (EOT; arithmetic mean 1,630 and

3,450 h ng⁻¹ ml⁻¹, respectively) than for 30 mg rentosertib BID (315 and 1,390 h ng⁻¹ ml⁻¹) and 30 mg rentosertib QD (553 and 788 h ng⁻¹ ml⁻¹) (Fig. 3d, Extended Data Fig. 5a and Supplementary Table 6). The steady state was achieved at week 2, and no obvious drug accumulation was observed by week 12. The geometric mean half-life ($t_{1/2}$) ranged from 10.9 to 12.0 h at week 12.

A higher AUC_{0-t} and $t_{1/2}$ at week 12 for all dosages indicates an increased exposure to rentosertib with increases time on treatment (Fig. 3a,c and Extended Data Fig. 5a,b). Change in patients' FVC from baseline to week 12 was positively correlated with AUC_{0-t} and trough concentration (C_{trough}) (Extended Data Fig. 5c,d). Not surprisingly, the C_{max} exposure was greatest in patients receiving the 60 mg QD dose, with both 30 mg QD and 30 mg BID showing similarly lower C_{max} (Fig. 3e), whereas C_{trough} was similar between 30 mg BID and 60 mg QD dosages (Fig. 3f). Together, the PK dynamics suggest that higher dosage leads to increased exposure from higher initial net absorption, with a more pronounced effect by the end of the treatment period associated with slower clearance.

Biomarkers and proteomic signatures of response in blood. We performed proteomic profiling of patient serum samples to understand the mechanism of action of rentosertib, guide development of biomarkers of response and evaluate the hypothesis that inhibition of TNIK may target biological aging[36]. We identified a total of 2,841 proteins using the Olink Explore 3072 panel across serum samples collected from patients in all treatment groups at baseline, 2 weeks, 4 weeks and 12 weeks. Using a linear regression model to evaluate time-dependent effects of rentosertib treatment on protein expression changes, we found that treatment duration substantially impacted protein expression patterns, with 20, 82 and 192 proteins significantly changing with treatment at weeks 2, 4 and 12, respectively (Benjamini–Hochberg-adjusted P value <0.1) (Extended Data Fig. 6a). Paired statistical testing to assess dose-associated changes in protein expression compared with placebo identified 1, 8 and 22 high-confidence (P_{adj} < 0.05) differentially abundant proteins in sera from patients receiving 30 mg QD, 30 mg BID and 60 mg QD rentosertib, respectively, using a generalized linear model (Fig. 4a,b and Supplementary Tables 7–9). Restricting analysis of differential proteins from baseline to week 12, the number of significantly altered proteins increased substantially with higher dosing: 0, 39 and 115 in the 30 mg QD, 30 mg BID and 60 mg QD groups, respectively (Extended Data Fig. 6b). Together, this suggests that the duration of

Table 1 | Characteristics of the patients at baseline

Characteristic	Rentosertib 30 mg QD *n*=18	Rentosertib 30 mg BID *n*=18	Rentosertib 60 mg QD *n*=18	Placebo *n*=17	Total *n*=71
Male sex – no. (%)	18 (100.0)	15 (83.3)	16 (88.9)	15 (88.2)	64 (90.1)
Age – years, mean ± s.d.	65.8±7.0	67.2±7.8	65.7±6.8	68.3±5.3	66.7±6.7
Race – no. (%)					
Asian	18 (100.0)	18 (100.0)	18 (100.0)	17 (100.0)	71 (100.0)
Weight – kg, mean ± s.d.	72.27±7.40	67.36±12.14	73.32±13.55	67.69±12.12	70.20±11.59
BMI – mean ± s.d.	25.66±2.08	24.41±3.40	26.41±4.13	24.96±3.73	25.36±3.43
Smoking or tobacco use history – no. (%)					
Never	5 (27.8)	4 (22.2)	6 (33.3)	5 (29.4)	20 (28.2)
Former	13 (72.2)	14 (77.8)	12 (66.7)	12 (70.6)	51 (71.8)
Current	0	0	0	0	0
Current antifibrotic treatment – no. (%)					
Nintedanib	6 (33.3)	4 (22.2)	9 (50.0)	3 (17.6)	22 (31.0)
Pirfenidone	5 (27.8)	4 (22.2)	2 (11.1)	4 (23.5)	15 (21.1)
FVC					
Minimum, maximum – ml	1,780, 3,413	1,486, 3,970	1,590, 3,710	1,331, 2,955	1,331, 3,970
Mean – ml, mean ± s.d.	2,696±444.2	2,617±667.4	2,762±684.2	2,246±473.6	2,585±600.4
Median – ml	2,707	2,563	2,784.5	2,181	2,637
Percent of predicted value – %, mean ± s.d.	73.6±12.8	75.9±16.0	78.5±21.0	66.5±12.6	73.7±16.3
DLCO					
Range – mmol min⁻¹ kPa⁻¹	2.475–6.437	1.580–5.025	1.985–6.130	1.595–5.635	1.580–6.437
Mean – mmol min⁻¹ kPa⁻¹, mean ± s.d.	3.783±1.035	3.429±0.932	3.756±1.253	3.608±1.087	3.645±1.069
Median – mmol min⁻¹ kPa⁻¹	3.628	3.375	3.601	3.648	3.589
Percent of predicted value (corrected) – %, mean±s.d.	48.0±12.8	45.4±10.8	48.3±16.0	48.9±16.1	47.6±13.8
LCQ total score – mean ± s.d.	17.129±3.089	16.168±3.519	15.743±3.701	16.437±3.050	16.368±3.322

rentosertib treatment and the dose are associated with changes in serum protein profiles.

Downregulated proteins associated with 30 mg BID and 60 mg QD treatment include known fibrosis-associated proteins such as MMP10, PTPRZ1, COL1A1, FAP, FN1, ROBO2, ASPN and LTBP2 (Fig. 4a–c and Supplementary Tables 7–10). Analyzing the differentially abundant proteins to find association with change in FVC found that ASPN, PTPRZ1, MMP10 and CHAD were both significantly inversely correlated to change in FVC ($P < 0.05$) and significantly downregulated after administration of rentosertib at the week 12 time point, suggesting an array of potential biomarkers for response to treatment (Fig. 4a–d and Supplementary Tables 7–9). Pathway enrichment analysis identified extracellular matrix organization as the most downregulated Reactome pathway gene set in both treatment groups, suggesting a reduction in excessive extracellular matrix production (Fig. 4e,f).

We queried diverse published gene expression datasets profiling the tissue of patients with IPF and that of healthy individuals using our AI-powered target discovery platform, PandaOmics[37], for expression patterns of these top genes to validate their relevance to IPF. *COL1A1*, *MMP10* and *FAP* were found to be universally upregulated in IPF patient samples compared with healthy individuals, and *FN1* was upregulated in most datasets (Extended Data Fig. 7a).

We further found that the abundance at week 12 of proteins previously reported to be associated with lung function[38] and transplant-free survival[39] in patients with IPF, such as ADAMTSL2, COL6A3, CCN3, COL24A1, KRT19 and LTBP2, were associated change in FVC (Extended Data Fig. 7b). The expression of inflammation-associated pathways,

other immune-related proteins, such as IL-10 and CD5, and other extracellular matrix-related proteins, such as COL6A3, were found to have significant associations with time on treatment and change in FVC, further suggesting that TNIK plays a diverse role in various aging-related dysregulated pathways[36] (Fig. 4e,f and Extended Data Fig. 8).

Discussion

In this phase 2a study, treatment with rentosertib at 30 mg QD, 30 mg BID and 60 mg QD over 12 weeks was safe and well tolerated. Treatment-related SAEs were rare, with a similarly low rate across treatment and placebo groups. The most common TEAEs leading to discontinuation of treatment were liver toxicity related and occurred mostly in patients who were also treated with nintedanib antifibrotic therapy, although notably not pirfenidone. In addition to liver toxicities, diarrhea and hypokalemia were among the most common TEAEs among participants treated with rentosertib. To determine the respective and synergistic contributions of rentosertib and SOC antifibrotic therapies to liver and gastrointestinal toxicity, as well as any potential effects on absorption or trough levels, we require further drug–drug interaction studies and assessment in a larger cohort of mixed SOC antifibrotic recipients and nonrecipients.
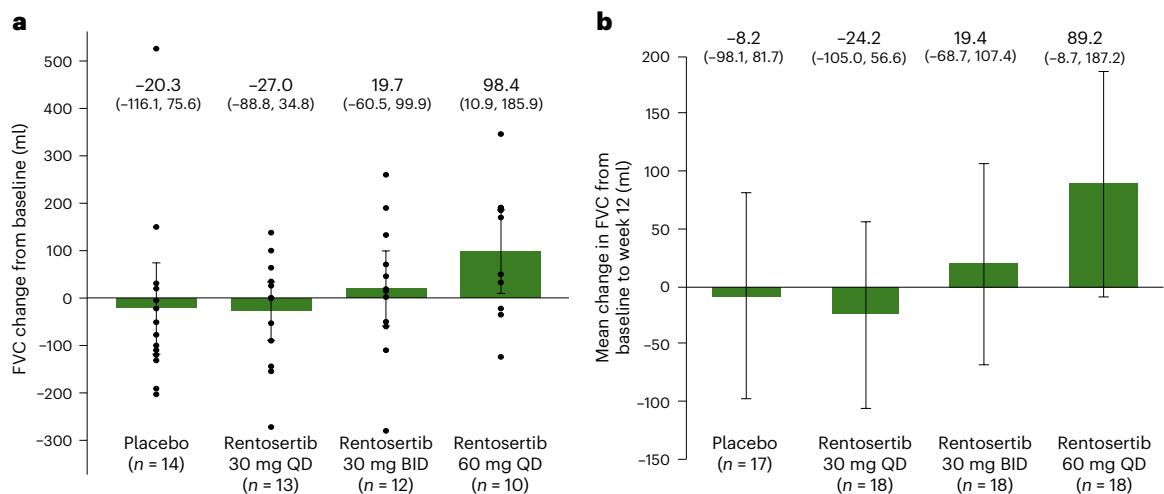
Treatment with 60 mg rentosertib QD over 12 weeks was associated with a trend toward an increase in FVC in patients with IPF. The 60 mg rentosertib QD dose exhibited the greatest mean improvement in lung function, as measured by FVC, whereas patients receiving placebo experienced an average decline in FVC. Patients receiving 60 mg rentosertib QD experienced a mean increase in FVC percentage change

Table 2 | AEs during treatment

Event	Rentosertib 30 mg QD n=18	Rentosertib 30 mg BID n=18	Rentosertib 60 mg QD n=18	Placebo n=17
Any AE – no. (%)	13 (72.2)	15 (83.3)	15 (83.3)	12 (70.6)
SAEs[a], grade ≥3 – no. (%)	2 (11.1)	4 (22.2)	7 (38.9)	3 (17.6)
Liver function				
Liver injury – no. (%)[b]	0 (0)	2 (11.1)	1 (5.6)	0 (0)
ALT increase – no. (%)	0 (0)	0 (0)	1 (5.6)	0 (0)
AST increase – no. (%)	0 (0)	0 (0)	1 (5.6)	0 (0)
SAEs resulting in death – no. (%)	0 (0)	1 (5.6)	0 (0)	0 (0)
AEs considered to be treatment related[c] – no. (%)	9 (50.0)	11 (61.1)	14 (77.8)	5 (29.4)
SAEs considered to be treatment related – no. (%)	1 (5.6)	2 (11.1)	2 (11.1)	0 (0)
AEs leading to treatment discontinuation[d] – no. (%)	1 (5.6)	5 (27.8)	4 (22.2)	2 (11.8)

[a]SAEs were defined as any AE resulting in death or that was life-threatening, required or prolonged hospitalization, resulted in persistent or substantial disability or incapacity, or was judged to jeopardize the subject and may have required medical or surgical intervention to prevent one of the other outcomes listed previously. [b]Liver injury defined as elevated ALT and/or AST ≥3-fold upper level of normal (ULN) combined with blood bilirubin ≥2-fold ULN or ALT and/or AST ≥10-fold ULN. Patients with liver injury are not counted among the totals for elevated ALT, AST or bilirubin individually. [c]AEs were defined as treatment related if the site investigator considered them definitely, probably or possibly related to treatment or with unknown or missing relationship to treatment. The most recent relationship was used when there were multiple records for the same AE. [d]Enrolled participants were considered for discontinuation of treatment if experiencing unacceptable AEs as determined by the site investigator, a need for concomitant medication(s) that interfere with the investigational drug or other study treatment and would constitute a safety hazard, an inability to receive study treatment for medical reason such as surgery, AEs or other diseases, unexplained weight loss if visit 2 BMI <18.5 kg m^{-2}, changes in ECG requiring intervention, or ECG QTcF >500 ms. See the study protocol, provided after request to the authors, for full criteria.

**Fig. 2 | Changes in FVC ± 95% CI after 12 weeks of rentosertib treatment compared to baseline. a**, The absolute change in FVC ± 95% CI. **b**, The absolute change in FVC ± 95% CI ANCOVA model with multiple imputation assuming missing at random (MAR).

of 2.82% by our modeling, meeting the minimal clinically important difference (MCID) reported for FVC in IPF of 2–6% (ref. 40). Subgrouping patients by concurrent SOC antifibrotic treatment showed patients receiving 60 mg rentosertib QD without SOC antifibrotic exhibited the strongest increase in FVC, suggesting potential interaction between the drugs that will be investigated in future trials. The incongruity of increased FVC with stable DLCO may be attributed to low numbers of patients in each treatment arm and the inherent variability of DLCO measurement[41].

The impact of rentosertib treatment on QOL metrics was largely inconclusive, with large variances within treatment arms, although our modeling found that patient-reported coughing-related QOL (via LCQ) was significantly improved in patients receiving 60 mg rentosertib QD. As various QOL metrics integrate the functionality of a number of organ systems, of which lung health is one contributing factor, a lack of difference among the treatment groups may be due to the relatively short data collection period and small cohort size.

AE-IPF is a strong indication of dismal patient prognosis[42] with a median survival of 2.2 months after onset[43], and incidence informs long-term therapeutic efficacy. Three acute exacerbations occurred in the 60 mg rentosertib arm and one in the placebo arm; however, a 12-week study is a relatively short time frame to capture such long-term disease events or trajectory[44]. An unintended consequence of rentosertib's potential immunomodulatory mechanism of action[9] may be a dampened site-specific immune response, potentially leading to increased susceptibility to infection, a known trigger for a subset of AE-IPF[45,46]. Because AE-IPF is a clinically important occurrence, we intend to assess its incidence in longer trials with larger cohorts in the future, which would assess patients for at least 12 months to more fully capture the incidence of AE-IPF and other potential AEs.

Assaying the serum proteome in patients provided insight into changes in circulating proteins associated with higher doses of rentosertib. The top up- and downregulated proteins showed high overlap
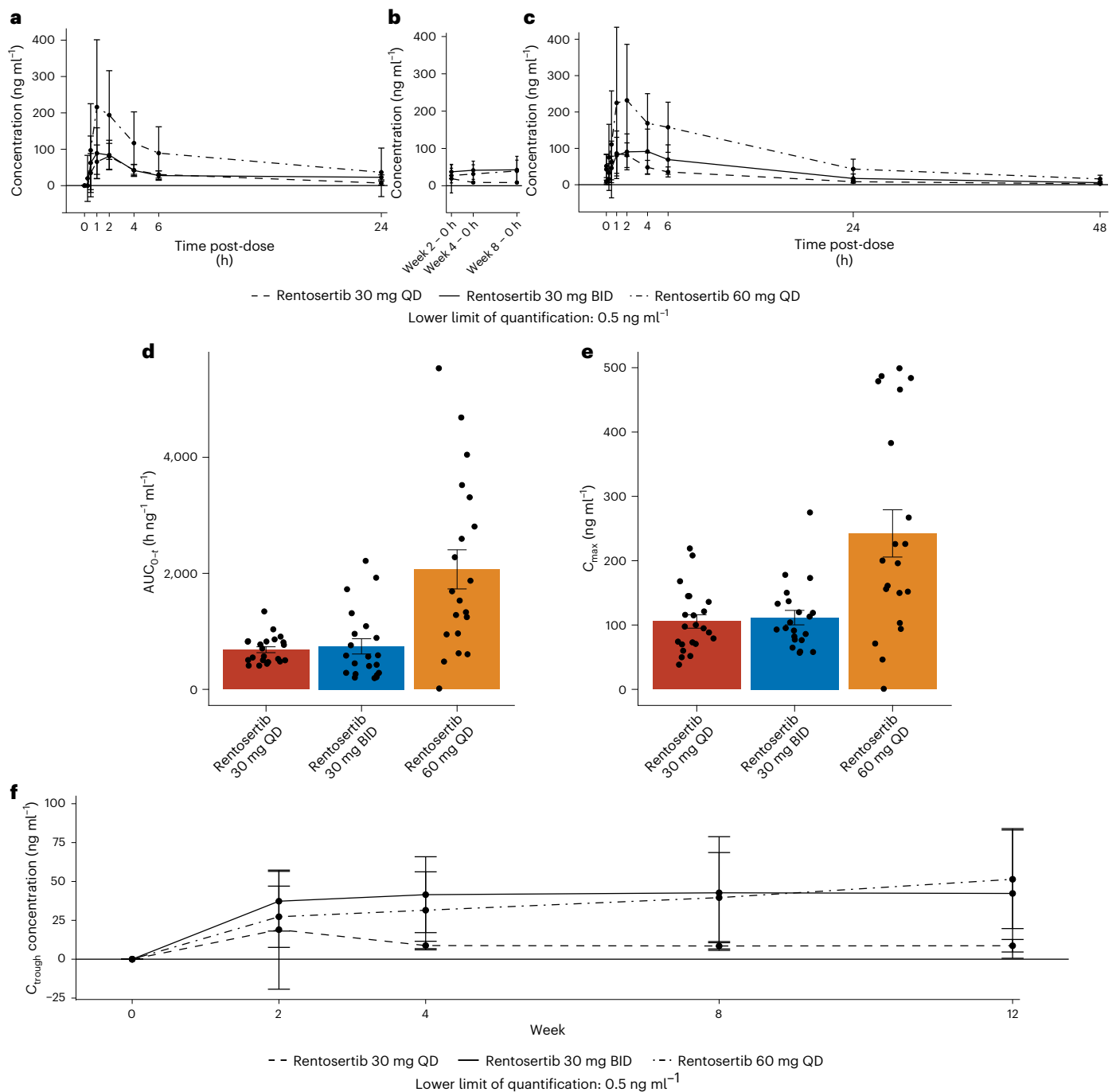
Fig. 3 | Pharmacokinetic properties of rentosertib. a–c, Pharmacokinetic dynamics of rentosertib in patient sera collected predose and periodically throughout 24 h posttreatment at week 0 (**a**), at 0 h posttreatment at weeks 2, 4 and 8 (**b**) and 48 h after administration at week 12 (**c**). **d**, AUC_{0-t} of rentosertib exposure; $n = 22$ in 30 mg QD, $n = 21$ in 30 mg BID, $n = 20$ in 60 mg QD. **e**, C_{max} of rentosertib exposure; $n = 22$ in 30 mg QD, $n = 21$ in 30 mg BID, $n = 20$ in 60 mg QD. **f**, C_{trough} of rentosertib exposure in patient sera collected pretreatment at weeks 0, 2, 4, 8 and 12. All data represent arithmetic mean ± s.d.

between the 30 mg BID and 60 mg QD doses, with downregulated proteins enriched for association with extracellular matrix organization, a key feature of fibrotic progression in IPF. Moreover, a number of the top downregulated proteins are known to be associated with pulmonary fibrosis: MMP10[47], LTBP2[39,48,49], KRT19[39] and COL24A1[39] have been nominated as biomarkers for IPF and transplant-free survival; PTPRZ1[50] activates β-catenin signaling, which contributes to IPF development[51], and BHLHE40 regulates epithelial-to-mesenchymal transition in IPF via β-catenin[52]; COL1A1 is a key component of dysregulated extracellular matrix deposition characteristic of fibrosis[53–55]; ASPN plays a role in myofibroblast transformation[56] and may play a central role in IPF

tissue remodeling[55,57]; circulating ROBO2 is associated with poor IPF prognosis[58]; FAP is expressed exclusively in fibrotic loci in the lungs of patients with IPF[59]; and CHAD binds to type II collagen in cartilaginous fibrotic loci[60,61]. Downregulation of this IPF-associated protein profile supports the hypothesis that inhibition of TNIK modulates IPF pathophysiological pathways and points to a potential serum protein signature as a biomarker for response to rentosertib treatment.

The limitations of this study include the small cohort size of each arm, the geographical and demographic homogeneity of the participants (all were residents of China of similar race) and a short period of follow-up, which limit the assessment of long-term safety
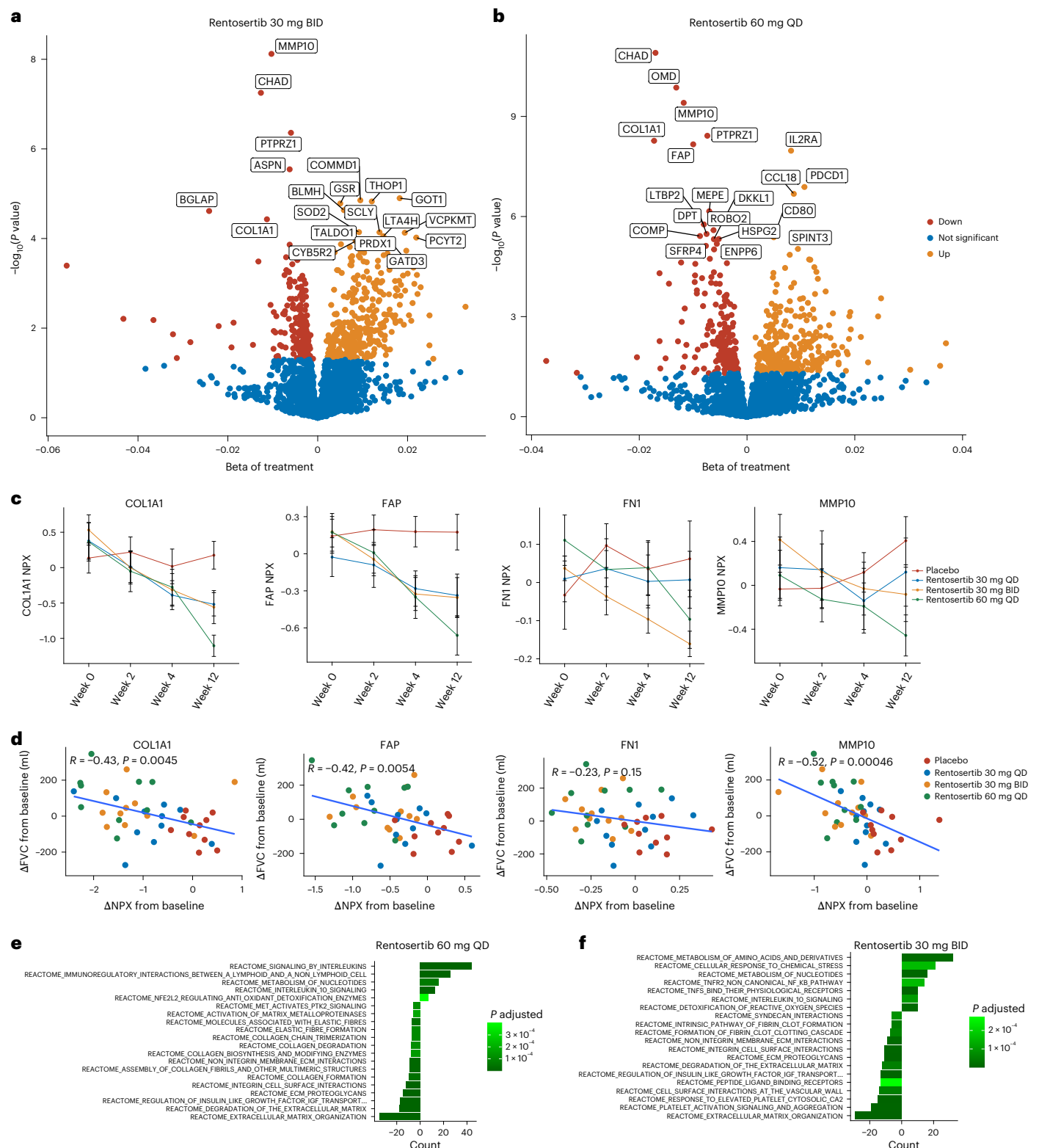
Fig. 4 | Post-hoc exploratory analysis of serum protein profiling.
a,**b**, Differentially abundant proteins in serum from patients receiving rentosertib at 30 mg BID (**a**) and 60 mg QD (**b**) identified with a generalized linear model. **c**, Serum levels of COL1A1, FAP, FN1 and MMP10 decrease with rentosertib dose and time on treatment. $n = 11$ patients in placebo, $n = 11$ patients in 30 QD, $n = 11$ patients in 30 BID, $n = 10$ patients in 60 QD. **d**, The changes in serum levels of COL1A1, FAP, FN1 and MMP10 from baseline to week 12 are inversely correlated with change in FVC from baseline to week 12. $n = 43$ patients at each visit; P value calculated by Pearson correlation analysis. **e**,**f**, Reactome pathway enrichment for differentially abundant proteins in serum from patients receiving rentosertib at 30 mg BID (**e**) and 60 mg QD (**f**).

and efficacy. Despite the short duration and the number of withdrawals from the trial across all arms ($n = 16/71$ (22.5%)), the results are encouraging for additional study of this drug candidate and target, suggesting that rentosertib is generally safe and potentially effective and, more broadly, that using AI in both target identification and in drug design may enhance the efficiency of the drug development process. Longer phase 2 or 3 trials studying rentosertib in a larger, heterogeneous sample of patients with IPF from around the globe are warranted to further evaluate the efficacy and safety of rentosertib treatment for IPF.

Online content

Any methods, additional references, Nature Portfolio reporting summaries, source data, extended data, supplementary information, acknowledgements, peer review information; details of author contributions and competing interests; and statements of data and code availability are available at https://doi.org/10.1038/s41591-025-03743-2.

References

1. Scannell, J. W., Blanckley, A., Boldon, H. & Warrington, B. Diagnosing the decline in pharmaceutical R&D efficiency. *Nat. Rev. Drug Discov.* **11**, 191–200 (2012).
2. Berdigaliyev, N. & Aljofan, M. An overview of drug discovery and development. *Future Med Chem.* **12**, 939–947 (2020).
3. Pun, F. W., Ozerov, I. V. & Zhavoronkov, A. AI-powered therapeutic target discovery. *Trends Pharmacol. Sci.* **44**, 561–572 (2023).
4. Qureshi, R. et al. AI in drug discovery and its clinical relevance. *Heliyon* **9**, e17575 (2023).
5. You, Y. et al. Artificial intelligence in cancer target identification and drug discovery. *Signal Transduct. Target. Ther.* **7**, 156 (2022).
6. Du, Y. et al. Machine learning-aided generative molecular design. *Nat. Mach. Intell.* **6**, 589–604 (2024).
7. Cheng, Y., Gong, Y., Liu, Y., Song, B. & Zou, Q. Molecular design in drug discovery: a comprehensive review of deep generative models. *Brief. Bioinform.* **22**, bbab344 (2021).
8. Sousa, T., Correia, J., Pereira, V. & Rocha, M. Generative deep learning for targeted compound design. *J. Chem. Inf. Model.* **61**, 5343–5361 (2021).
9. Ren, F. et al. A small-molecule TNIK inhibitor targets fibrosis in preclinical and clinical models. *Nat. Biotechnol.* https://doi.org/10.1038/s41587-024-02143-0 (2024).
10. Xu, J. et al. Discovery of a novel and potent cyclin-dependent kinase 8/19 (CDK8/19) inhibitor for the treatment of cancer. *J. Med. Chem.* **67**, 8161–8171 (2024).
11. Aliper, A. et al. Prediction of clinical trials outcomes based on target choice and clinical trial design with multi-modal artificial intelligence. *Clin. Pharmacol. Ther.* **114**, 972–980 (2023).
12. Feuerriegel, S. et al. Causal machine learning for predicting treatment outcomes. *Nat. Med.* **30**, 958–968 (2024).
13. Feijoo, F., Palopoli, M., Bernstein, J., Siddiqui, S. & Albright, T. E. Key indicators of phase transition for clinical trials through machine learning. *Drug Discov. Today* **25**, 414–421 (2020).
14. Artemov, A. V. et al. Integrated deep learned transcriptomic and structure-based predictor of clinical trials outcomes. Preprint at *bioRxiv* https://doi.org/10.1101/095653 (2016).
15. Gayvert, K. M., Madhukar, N. S. & Elemento, O. A data-driven approach to predicting successes and failures of clinical trials. *Cell Chem. Biol.* **23**, 1294–1301 (2016).
16. Lavecchia, A. Navigating the frontier of drug-like chemical space with cutting-edge generative AI models. *Drug Discov. Today* **29**, 104133 (2024).
17. Jiménez-Luna, J., Grisoni, F., Weskamp, N. & Schneider, G. Artificial intelligence in drug discovery: recent advances and future perspectives. *Expert Opin. Drug Discov.* **16**, 949–959 (2021).
18. Mak, K.-K. & Pichika, M. R. Artificial intelligence in drug development: present status and future prospects. *Drug Discov. Today* **24**, 773–780 (2019).
19. Jayatunga, M. K. P., Xie, W., Ruder, L., Schulze, U. & Meier, C. AI in small-molecule drug discovery: a coming wave? *Nat. Rev. Drug Discov.* **21**, 175–176 (2022).
20. Wong, C. H., Siah, K. W. & Lo, A. W. Estimation of clinical trial success rates and related parameters. *Biostatistics* **20**, 273–286 (2019).
21. KP Jayatunga, M., Ayers, M., Bruens, L., Jayanth, D. & Meier, C. How successful are AI-discovered drugs in clinical trials? A first analysis and emerging lessons. *Drug Discov. Today* **29**, 104009 (2024).
22. Pun, F. W. et al. Identification of therapeutic targets for amyotrophic lateral sclerosis using PandaOmics—an AI-enabled biological target discovery platform. *Front. Aging Neurosci.* **14**, 914017 (2022).
23. Pun, F. W. et al. Hallmarks of aging-based dual-purpose disease and age-associated targets predicted using PandaOmics AI-powered discovery engine. *Aging* **14**, 2475–2506 (2022).
24. Raghu, G. et al. Diagnosis of idiopathic pulmonary fibrosis. An official ATS/ERS/JRS/ALAT clinical practice guideline. *Am. J. Respir. Crit. Care Med.* **198**, e44–e68 (2018).
25. Lederer, D. J. & Martinez, F. J. Idiopathic pulmonary fibrosis. *N. Engl. J. Med.* **378**, 1811–1823 (2018).
26. Richeldi, L., Collard, H. R. & Jones, M. G. Idiopathic pulmonary fibrosis. *Lancet* **389**, 1941–1952 (2017).
27. Raghu, G. & Richeldi, L. Current approaches to the management of idiopathic pulmonary fibrosis. *Respir. Med.* **129**, 24–30 (2017).
28. Martinez, F. J. et al. Idiopathic pulmonary fibrosis. *Nat. Rev. Dis. Prim.* **3**, 17074 (2017).
29. Raghu, G. Idiopathic pulmonary fibrosis: lessons from clinical trials over the past 25 years. *Eur. Respir. J.* **50**, 1701209 (2017).
30. King, T. E., Tooze, J. A., Schwarz, M. I., Brown, K. R. & Cherniack, R. M. Predicting survival in idiopathic pulmonary fibrosis. *Am. J. Respir. Crit. Care Med.* **164**, 1171–1181 (2001).
31. Wollin, L. et al. Mode of action of nintedanib in the treatment of idiopathic pulmonary fibrosis. *Eur. Respir. J.* **45**, 1434–1445 (2015).
32. Aimo, A. et al. Pirfenidone for idiopathic pulmonary fibrosis and beyond. *Card. Fail Rev.* **8**, e12 (2022).
33. Noble, P. W. et al. Pirfenidone in patients with idiopathic pulmonary fibrosis (CAPACITY): two randomised trials. *Lancet* **377**, 1760–1769 (2011).
34. Richeldi, L. et al. Efficacy and safety of nintedanib in idiopathic pulmonary fibrosis. *N. Engl. J. Med.* **370**, 2071–2082 (2014).
35. King, T. E. et al. A phase 3 trial of pirfenidone in patients with idiopathic pulmonary fibrosis. *N. Engl. J. Med.* **370**, 2083–2092 (2014).
36. Ewald, C. Y. et al. TNIK's emerging role in cancer, metabolism, and age-related diseases. *Trends Pharmacol. Sci.* **45**, 478–489 (2024).
37. Kamya, P. et al. PandaOmics: an AI-driven platform for therapeutic target and biomarker discovery. *J. Chem. Inf. Model.* **64**, 3961–3969 (2024).
38. Su, C.-Y. et al. Multi-ancestry proteome-phenome-wide Mendelian randomization offers a comprehensive protein-disease atlas and potential therapeutic targets. Preprint at *medRxiv* https://doi.org/10.1101/2024.10.17.24315553 (2024).
39. Oldham, J. M. et al. Proteomic biomarkers of survival in idiopathic pulmonary fibrosis. *Am. J. Respir. Crit. Care Med.* **209**, 1111–1120 (2024).
40. du Bois, R. M. et al. Forced vital capacity in patients with idiopathic pulmonary fibrosis: test properties and minimal clinically important difference. *Am. J. Respir. Crit. Care Med.* **184**, 1382–1389 (2011).

41. McCormack, M. C. Facing the noise: addressing the endemic variability in DLCO testing. *Respir. Care* **57**, 17–25 (2012).

42. Collard, H. R. et al. Acute exacerbations of idiopathic pulmonary fibrosis. *Am. J. Respir. Crit. Care Med.* **176**, 636–643 (2007).

43. Song, J. W., Hong, S.-B., Lim, C.-M., Koh, Y. & Kim, D. S. Acute exacerbation of idiopathic pulmonary fibrosis: incidence, risk factors and outcome. *Eur. Respir. J.* **37**, 356–363 (2011).

44. Richeldi, L. et al. Trial of a preferential phosphodiesterase 4B inhibitor for idiopathic pulmonary fibrosis. *N. Engl. J. Med.* **386**, 2178–2187 (2022).

45. Wootton, S. C. et al. Viral infection in acute exacerbation of idiopathic pulmonary fibrosis. *Am. J. Respir. Crit. Care Med.* **183**, 1698–1702 (2011).

46. Collard, H. R. et al. Acute exacerbation of idiopathic pulmonary fibrosis. An International Working Group Report. *Am. J. Respir. Crit. Care Med.* **194**, 265–275 (2016).

47. Sokai, A. et al. Matrix metalloproteinase-10: a novel biomarker for idiopathic pulmonary fibrosis. *Respir. Res.* **16**, 120 (2015).

48. Enomoto, Y. et al. LTBP2 is secreted from lung myofibroblasts and is a potential biomarker for idiopathic pulmonary fibrosis. *Clin. Sci.* **132**, 1565–1580 (2018).

49. Zou, M. et al. Plasma LTBP2 as a potential biomarker in differential diagnosis of connective tissue disease-associated interstitial lung disease and idiopathic pulmonary fibrosis: a pilot study. *Clin. Exp. Med.* **23**, 4809–4816 (2023).

50. Shang, D., Xu, X., Wang, D., Li, Y. & Liu, Y. Protein tyrosine phosphatase ζ enhances proliferation by increasing β-catenin nuclear expression in VHL-inactive human renal cell carcinoma cells. *World J. Urol.* **31**, 1547–1554 (2013).

51. Chilosi, M. et al. Aberrant Wnt/β-catenin pathway activation in idiopathic pulmonary fibrosis. *Am. J. Pathol.* **162**, 1495–1502 (2003).

52. Hu, X. et al. Dec1 deficiency ameliorates pulmonary fibrosis through the PI3K/AKT/GSK-3β/β-catenin integrated signaling pathway. *Front. Pharmacol.* **13**, 829673 (2022).

53. Devos, H., Zoidakis, J., Roubelakis, M. G., Latosinska, A. & Vlahou, A. Reviewing the regulators of COL1A1. *Int. J. Mol. Sci.* **24**, 10004 (2023).

54. Bibaki, E. et al. miR-185 and miR-29a are similarly expressed in the bronchoalveolar lavage cells in IPF and lung cancer but common targets DNMT1 and COL1A1 show disease specific patterns. *Mol. Med. Rep.* **17**, 7105–7112 (2018).

55. Wan, H. et al. Identification of Hub genes and pathways associated with idiopathic pulmonary fibrosis via bioinformatics analysis. *Front. Mol. Biosci.* **8**, 711239 (2021).

56. Huang, S. et al. Asporin promotes TGF-β–induced lung myofibroblast differentiation by facilitating Rab11-dependent recycling of TβRI. *Am. J. Respir. Cell Mol. Biol.* **66**, 158–170 (2022).

57. Åhrman, E. et al. Quantitative proteomic characterization of the lung extracellular matrix in chronic obstructive pulmonary disease and idiopathic pulmonary fibrosis. *J. Proteom.* **189**, 23–33 (2018).

58. Todd, J. L. et al. Association of circulating proteins with death or lung transplant in patients with idiopathic pulmonary fibrosis in the IPF-PRO Registry Cohort. *Lung* **200**, 11–18 (2022).

59. Acharya, P. S., Zukas, A., Chandan, V., Katzenstein, A.-L. A. & Puré, E. Fibroblast activation protein: a serine protease expressed at the remodeling interface in idiopathic pulmonary fibrosis. *Hum. Pathol.* **37**, 352–360 (2006).

60. Hoffman, E. T. et al. Regional and disease specific human lung extracellular matrix composition. *Biomaterials* **293**, 121960 (2023).

61. Shum, L. Chondroadherin binds to type II collagen. *Arthritis Res. Ther.* **3**, 72650 (2001).

Zuojun Xu [iD] [1] ✉, **Feng Ren** [iD] [2], **Ping Wang**[1], **Jie Cao**[3], **Chunting Tan**[4], **Dedong Ma**[5], **Li Zhao**[6], **Jinghong Dai**[7], **Yipeng Ding**[8], **Haohui Fang**[9], **Huiping Li** [iD] [10], **Hong Liu**[11], **Fengming Luo**[12], **Ying Meng**[13], **Pinhua Pan**[14], **Pingchao Xiang**[15], **Zuke Xiao**[16], **Sujata Rao**[17], **Carol Satler**[17], **Sang Liu**[2], **Yuan Lv**[2], **Heng Zhao**[2], **Shan Chen**[2], **Hui Cui**[2], **Mikhail Korzinkin**[18], **David Gennert** [iD] [17] & **Alex Zhavoronkov** [iD] [2,17,18,19] ✉

[1]Department of Pulmonary and Critical Care Medicine, Peking Union Medical College Hospital, Beijing, China. [2]Insilico Medicine Shanghai, Shanghai, China. [3]Department of Respiratory and Critical Care Medicine, Tianjin Medical University General Hospital, Tianjin, China. [4]Department of Pulmonary and Critical Care Medicine, Beijing Friendship Hospital, Capital Medical University, Beijing, China. [5]Department of Respiratory Disease, Qilu Hospital of Shandong University, Jinan, China. [6]Department of Respiratory Medicine, Shengjing Hospital of China Medical University, Shenyang, China. [7]Department of Pulmonary and Critical Care Medicine, Nanjing Drum Tower Hospital, Nanjing University, Nanjing, China. [8]Department of Respiratory and Critical Care Medicine, Hainan General Hospital, Haikou, China. [9]Department of Respiratory and Critical Care, Anhui Chest Hospital, Hefei, China. [10]Department of Respiratory Medicine, Shanghai Pulmonary Hospital, Tongji University, Shanghai, China. [11]Department of Respiratory and Critical Care Medicine, The First Affiliated Hospital of Zhengzhou University, Zhengzhou, China. [12]Department of Pulmonary and Critical Care Medicine, West China Hospital, Sichuan University, Chengdu, China. [13]Department of Respiratory and Critical Care Medicine, Nanfang Hospital, Southern Medical University, Guangzhou, China. [14]Department of Respiratory Medicine, Xiangya Hospital, Central South University, Changsha, China. [15]Department of Respiratory and Critical Care Medicine, Peking University Shougang Hospital, Beijing, China. [16]Department of Respiratory and Critical Care Medicine, Jiangxi Provincial People's Hospital, Nanchang, China. [17]Insilico Medicine US, Cambridge, MA, USA. [18]Insilico Medicine AI, Abu Dhabi, United Arab Emirates. [19]Insilico Medicine Hong Kong, Hong Kong SAR, China. ✉e-mail: xuzj@hotmail.com; alex@insilico.com

Methods

Study design

This phase 2a, multicenter, double-blind, placebo-controlled, randomized, multidose trial of rentosertib in adults with IPF was performed at 21 sites across China beginning 19 July 2023 and running through 11 June 2024. Adults with IPF were randomly assigned in a 1:1:1:1 ratio via interactive response technology to receive oral rentosertib (at a dose of 30 mg (QD), 30 mg (BID) or 60 mg (QD)) or placebo (QD) for 12 weeks, along with the continued use of SOC medications (Fig. 1). Patient screening occurred, on average, 30 days before the first dosing at the second visit. Patients were clinically evaluated on day 1, week 2, week 4, week 8, week 12 (end of treatment) and week 13 (end of study). The study treatment rentosertib was provided by Insilico Medicine or a designated contract research organization, packaged and labeled in accordance with the principles of Good Manufacturing Practice. Resupply to the sites was managed via an interactive response technology system, which also monitored expiry dates of supplies available at the sites. Access to the randomization codes was controlled and documented.

The trial was conducted following the principles outlined in the Declaration of Helsinki and the International Council for Harmonization guidelines for Good Clinical Practice. The institutional review board or ethics committee at participating centers approved protocols and adhered to local laws before initiation of the clinical trial. All patients in this study provided written informed consent. Trial management and data processing, summarization and analyses were conducted by Fortrea Clinical Pharmacology Services, Leeds, UK.

Authors used by the study sponsor were involved in the trial design, collection, analysis and data interpretation. Subjects, investigators, site study staff, reviewers and everyone involved in study conduct or analysis were blinded with regard to the randomized treatment assignments until after data freeze. Bioanalytics staff were allowed to identify samples from subjects assigned to placebo treatment but did not disclose randomization until trial unblinding. These authors contributed to manuscript preparation across all iterations of the manuscript. The first and last authors of this study vouch for the completeness of all data reported in this publication.

Participants

Eligible patients were 40 years of age or older with an IPF diagnosis as defined by the American Thoracic Society, European Respiratory Society, Japanese Respiratory Society and Latin American Thoracic Association guidelines[62]. Enrolled patients presented with stable IPF and were deemed suitable for study participation on the basis of medical history, physical examination, vital signs, 12-lead ECG and laboratory evaluation. Patients previously receiving nintedanib or pirfenidone were enrolled if their antifibrotic therapy had been stable for >8 weeks before the first (screening) visit. Eligible patients had to meet all three of the following criteria during the screening visit: (1) FVC >40% predicted of normal, (2) DLCO corrected for hemoglobin ≥25% and <80% predicted of normal, and (3) FEV1/FVC ratio >0.7 based on prebronchodilator value. Patients were excluded for concomitant respiratory disorders or health concerns, including, but not limited to, cystic fibrosis, active aspergillosis, active tuberculosis, confirmed coronavirus disease 2019 (COVID-19) at visits 1 or 2 or severe COVID-19 requiring hospitalization within 6 months of visit 1 or long COVID-19, clinically relevant or severe pulmonary hypertension, acute IPF exacerbation within 4 months before visit 1 and/or during the screening period, upper or lower respiratory tract infection that has not fully resolved within 4 weeks before visit 1 and/or before visit 2 (day 1), active on the lung transplantation register or expected to become active on the lung transplant register within 6 months before visit 1, a history of lung volume reduction surgery or lung transplant, current smoker, BMI >40 kg m^{-2}, aspartate aminotransferase (AST) or ALT ≥1.5 times upper level of normal or total bilirubin ≥1.5 times upper level of normal at visit 1, eGFR ≤60 ml min^{-1} 1.73 m^{-2} (Chronic Kidney Disease Epidemiology Collaboration formula) at visit 1, uncontrolled hypertension (systolic pressure >160 mmHg or diastolic pressure >95 mmHg despite treatment with antihypertensive treatments) at visit 1, unstable cardiac angina or myocardial infarction within 6 months before visit 1, taking oral corticosteroids, any documented active or suspected malignancy or history of malignancy within 5 years before visit 1, known hypersensitivity or contraindications to serine/threonine kinase inhibitors, any condition or treatment possibly affecting drug absorption (for example, gastrectomy or metoclopramide), taking restricted medications (for example, moderate-to-strong CYP3A4–CYP1A2 inhibitors or inducers or medications primarily metabolized by CYP3A4–CYP1A2) or consumption of grapefruit or grapefruit juice, pomelo, Seville orange or Seville orange-containing products within 48 h before day 1, substantial trauma or major surgery within 3 months before visit 1 or planned major surgery during the study and 12-lead ECG demonstrating corrected QT interval by Fridericia (QTcF) >450 ms for males and >470 ms for females, or a QRS interval >120 ms at visit 1. Full inclusion and exclusion criteria are detailed in the associated study protocol.

Given an approximate sample size of 15 subjects per treatment arm, there exists a 90% probability of observing at least one AE if the true population rate is approximately 15%, which is sufficient to assess the feasibility of safety parameters.

Objectives and endpoints

The primary objective of this study was to evaluate the safety and tolerability of orally administered rentosertib for up to 12 weeks in adult patients with IPF compared with placebo. The primary endpoint for this study was the percentage of patients who have at least one TEAE. Patients were continually monitored for AEs during the 12 weeks of rentosertib treatment and for 1 week after administration of the final dose, with study drug-related SAE and AEs of special interest collected if they occurred beyond the study period.

The secondary efficacy endpoints measured the relative and percent change in FVC from week 0/visit 2 up to week 12. The absolute and relative change in FVC (%) predicted from week 0/visit 2 up to week 12 as well as the change in DLCO (%) predicted from week 0 up to week 12 was also measured. Twenty-one subjects (29.6%) had FVC and FEV1 measured at baseline (randomization with spirometry equipment sourced from the local site meeting the 2019 American Thoracic Society and European Respiratory Society guideline criteria)[63], provided that the subject's baseline and end-of-treatment spirometry were performed with the same equipment. Fifty subjects (70.4%) had FVC and FEV1 measured at baseline/randomization with centrally sourced SpiroSphere devices (Clario) provided by the sponsor with study-specific training and proficiency tests to the operating staff to meet the 2019 ATS/ERS guideline criteria[63] with central overread. All DLCO measurements were assessed with devices from each site according to the ATS/ERS guidelines[64], and all measurements were conducted with the same equipment for each site. FVC MCID has been reported to be a change of 2–6% in patients with IPF[40].

The change in LCQ, a 19-item questionnaire that assesses cough-related QOL[65], from week 0 to weeks 4, 8 and 12 was also analyzed. The LCQ examines three domains (physical, psychological and social) related to the patient's experience within a 24-h time frame. The range for the total score on the LCQ is 3–21, with the sum of each domain score ranging from 1 to 7. A higher score indicates a better QOL, with an MCID reported to be a change of 1.3 points for patients with chronic obstructive pulmonary disease[66]. The LCQ questionnaire has mainly been validated in disease settings such as chronic obstructive pulmonary disease[67], noncystic fibrosis bronchiectasis[68] and chronic cough[69].

The change in 6MWD in meters from week 0 to week 12 was also evaluated.

Other secondary endpoints included pharmacokinetic parameters of rentosertib and related metabolites after the first dose at visit 2 and the last dose at visit 6 (EOT). This study also collected data on the number of acute IPF exacerbations and the number of days hospitalized after acute IPF exacerbations from week 0 through week 12.

The exploratory endpoints analyzed include the change in IPF blood biomarkers after rentosertib treatment at weeks 0, 2, 4, 8 and 12. Changes in the blood proteome in treated patients were also measured at weeks 0, 2, 4, 8 and 12.

Statistical analysis

An analysis of covariance (ANCOVA) model was performed for endpoints including FVC. The model includes treatment as a fixed effect and baseline value as a covariate. LCQ scores were analyzed using a mixed model for repeated measures. FVC and other spirometry measurements were collected at baseline and at week 12, with all patients being measured at baseline and a total of 22 patients missing week 12 measurements (5 receiving 30 mg rentosertib QD, 6 receiving 30 mg rentosertib BID, 8 receiving 60 mg rentosertib QD and 3 receiving placebo). Missing values at week 12 were imputed using a multiple imputation method assuming missing at random. All statistical comparisons were made using two-sided tests. No statistical comparisons of AEs between treatment groups were performed. Given an approximate sample size of 15 subjects per treatment arm, there exists a 90% probability of observing at least one AE if the true population rate is approximately 15%, which was sufficient to assess the feasibility of safety parameters, although a sample size calculation based on statistical power considerations was not performed. Spearman correlation analysis was used to assess the association between FVC change and AUC_{0-t} or C_{trough}.

The safety population included all subjects who received at least one dose of study treatment. The intent-to-treat population included any randomized subjects. The intent-to-treat population was used for summary of demographic and baseline characteristics and for analysis of secondary endpoints, except PK analysis. Assessment of PK parameters included subjects who received at least one dose of study treatment and had at least one measurable concentration collected after dosing. Assessment of serum biomarkers was performed on subjects who had a predose baseline value and at least one value after treatment initiated.

For Olink proteomics analyses, we utilized a generalized linear mixed model to assess the association between each protein and dose or FVC change. The formula for modeling the treatment effect is

$$\text{NPX (protein level)} \approx \text{treatment} + \text{visit} + \text{treatment} : \text{visit} + (1|\text{PatientID})$$

The lme4 package was used for the generalized linear mixed model analysis. For modeling the FVC changes, we conducted the statistical analyses in two steps. In the first step, we regressed the protein level (NPX) against the visit to obtain the slope of protein change rate for each individual. In the second step, we regressed the FVC changes against the slope of protein change rates obtained from the first step. This was conducted using the lm package. Pathway analyses were performed using the clusterProfiler R package, with Reactome processes[70] as the curated pathway set.

Reporting summary

Further information on research design is available in the Nature Portfolio Reporting Summary linked to this article.

Data availability

Complete deidentified Olink proteomics data, and FVC data, have been deposited at the OMIX database under accession codes at OMIX008341 (https://ngdc.cncb.ac.cn/omix/release/OMIX008341).

Qualified researchers may request access to Olink proteomics data through the OMIX database at https://ngdc.cncb.ac.cn/omix/. Study protocol and statistical analysis plan will be provided in a secure data sharing environment upon academic or research request. Source data are provided with this paper.

Code availability

Custom code used to analyze Olink proteomics data is available via GitHub at https://github.com/HUICUI1992/Code-for-NM.

References

62. Raghu, G. et al. Idiopathic pulmonary fibrosis (an update) and progressive pulmonary fibrosis in adults: an official ATS/ERS/JRS/ALAT clinical practice guideline. *Am. J. Respir. Crit. Care Med.* **205**, e18–e47 (2022).
63. Graham, B. L. et al. Standardization of Spirometry 2019 Update. An Official American Thoracic Society and European Respiratory Society Technical Statement. *Am. J. Respir. Crit. Care Med.* **200**, e70–e88 (2019).
64. Graham, B. L. et al. 2017 ERS/ATS standards for single-breath carbon monoxide uptake in the lung. *Eur. Respir. J.* **49**, 1600016 (2017).
65. Birring, S. S. et al. Development of a symptom specific health status measure for patients with chronic cough: Leicester Cough Questionnaire (LCQ). *Thorax* https://doi.org/10.1136/thorax.58.4.339 (2003).
66. Rebelo, P. et al. Minimal clinically important differences for patient-reported outcome measures of cough and sputum in patients with COPD. *Int. J. Chron. Obstruct. Pulmon. Dis.* **15**, 201–212 (2020).
67. Berkhof, F. F. et al. The validity and precision of the Leicester Cough Questionnaire in COPD patients with chronic cough. *Health Qual. Life Outcomes* **10**, 4 (2012).
68. Murray, M. P., Turnbull, K., MacQuarrie, S., Pentland, J. L. & Hill, A. T. Validation of the Leicester Cough Questionnaire in non-cystic fibrosis bronchiectasis. *Eur. Respir. J.* **34**, 125–131 (2009).
69. Nguyen, A. M. et al. Leicester Cough Questionnaire validation and clinically important thresholds for change in refractory or unexplained chronic cough. *Ther. Adv. Respir. Dis.* **16**, 17534666221099737 (2022).
70. Milacic, M. et al. The Reactome Pathway Knowledgebase 2024. *Nucleic Acids Res.* **52**, D672–D678 (2024).

Author contributions

A.Z., Z.X., P.W., F.R. and S.R. conceived and designed the clinical study. Z.X., P.W., J.C., C.T., D.M., L.Z., J.D., Y.D., H.F., H. Li, H. Liu, F.L., Y.M., P.P., P.X. and Z.X. participated in patient enrollment, carried out the trial and acquired data. S.L., Y.L., H.Z., S.C., H.C., C.S., M.K., D.G., F.R. and A.Z. analyzed and interpreted the data. D.G., S.L., Y.L., H.Z., S.C., H.C., C.S. and A.Z. wrote and revised the paper. All authors have seen and approved of the paper before submission.

Competing interests

F.R., S.R., C.S., S.L., Y.L., H.Z., S.C., H.C., M.K., D.G. and A.Z. are employees of Insilico Medicine. Insilico Medicine was the study sponsor. The other authors declare no competing interests.

Additional information

**Extended data** is available for this paper at
https://doi.org/10.1038/s41591-025-03743-2.

Supplementary information The online version contains supplementary
material available at https://doi.org/10.1038/s41591-025-03743-2.

Correspondence and requests for materials should be addressed to
Zuojun Xu or Alex Zhavoronkov.

Peer review information *Nature Medicine* thanks Yuben Moodley,
Luca Richeldi, Jeff Swigris and the other, anonymous, reviewer(s) for
their contribution to the peer review of this work. Primary Handling
Editor: Lorenzo Righetto, in collaboration with the *Nature Medicine*
team.

Reprints and permissions information is available at
www.nature.com/reprints.
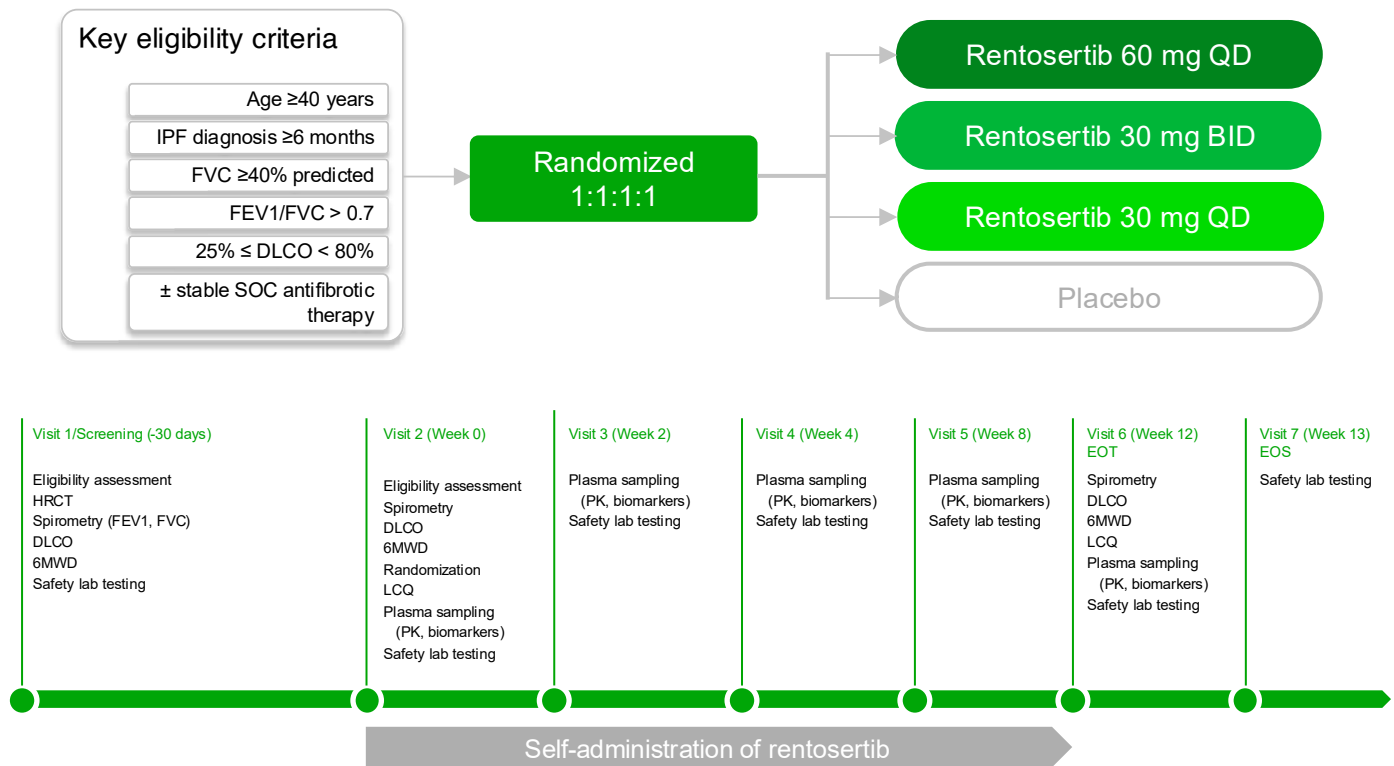
Extended Data Fig. 1 | Key trial eligibility criteria, randomization scheme, and schedule of key study activities. Eligible patients were randomized to receive 30 mg rentosertib QD, 30 mg rentosertib BID, 60 mg rentosertib QD, or placebo administered over 12 weeks with periodic assessment and plasma sampling. IPF, idiopathic pulmonary fibrosis; FVC, forced vital capacity; FEV1, forced expiratory volume in one second; DLCO, diffusion capacity of the lung for carbon monoxide; SOC, standard-of-care; QD, once-daily; BID, twice-daily; HRCT, high-resolution computed tomography; 6MWD, six-minute walk distance; LCQ, Leicester cough questionnaire; PK, pharmacokinetics; EOT, end-of-trial; EOS, end-of-study.

Extended Data Fig. 2 | See next page for caption.

Extended Data Fig. 2 | Changes in FVC after 12 weeks of treatment with rentosertib. a-b) Changes in forced vital capacity (FVC) ± 95% CI after 12 weeks of treatment compared to baseline excluding n = 1 patient from the placebo group and n = 1 patient from the rentosertib 30 mg QD group who exhibited >600 mL difference between screening and baseline FVC measurements, making uncertain the baseline FVC values in those patients. Absolute change in FVC ± 95% CI (**a**) and absolute change in FVC ± 95% CI ANCOVA Model with Multiple Imputation assuming missing at random (MAR) (**b**). (**c**) Absolute change in FVC (% Predicted) ± SE, ANCOVA Model with Multiple Imputation assuming MAR. (**d**) Percentage change in FVC ± SE, ANCOVA Model with Multiple Imputation assuming MAR. (**e**) Change in percent predicted FVC ± SD.
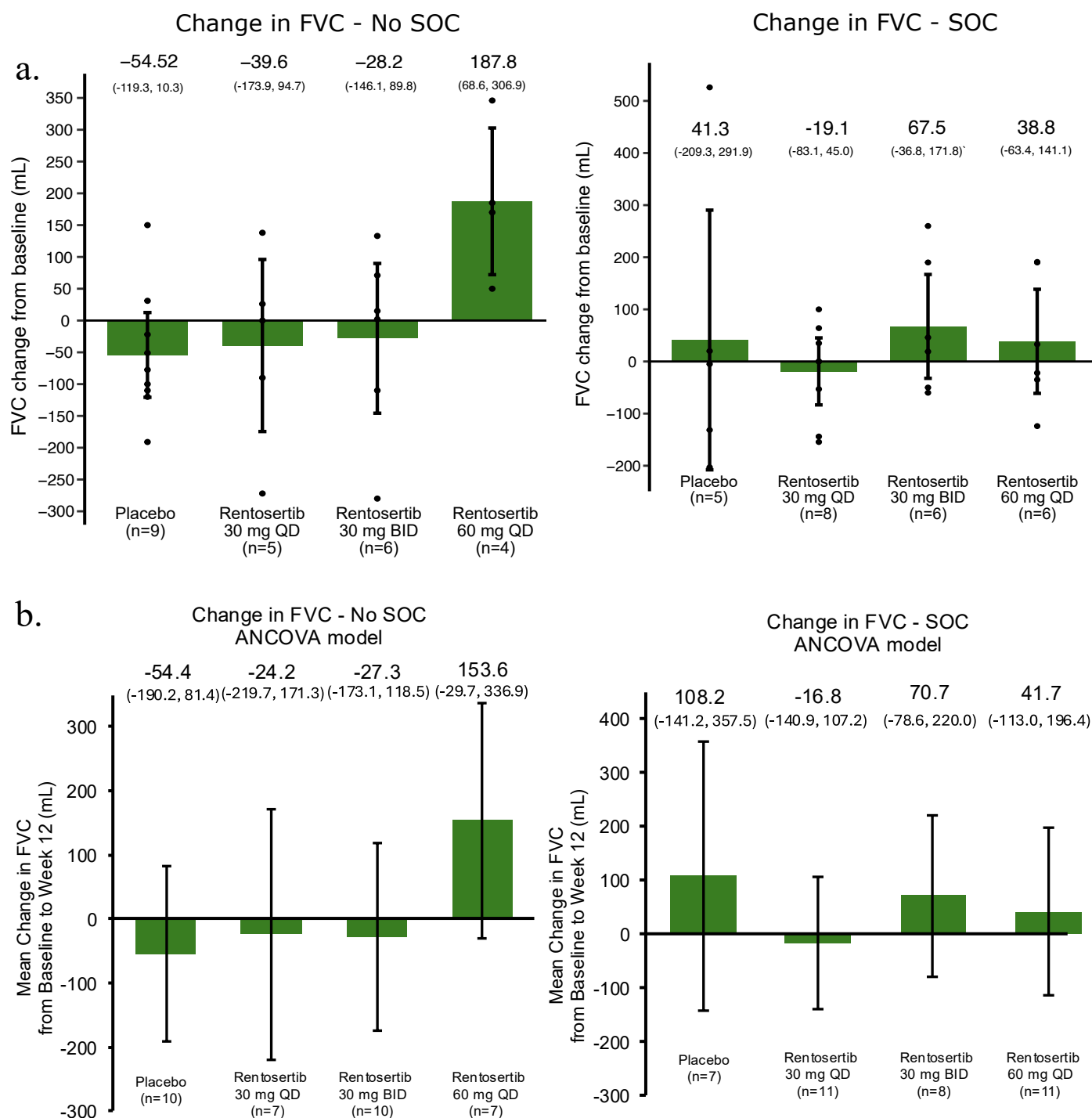
Extended Data Fig. 3 | Changes in FVC after 12 weeks of treatment with rentosertib stratified by concurrent use of SOC antifibrotic therapy. (a) Absolute change in FVC ± 95% CI in patients not concurrently taking SOC antifibrotic therapy (left) or in patients concurrent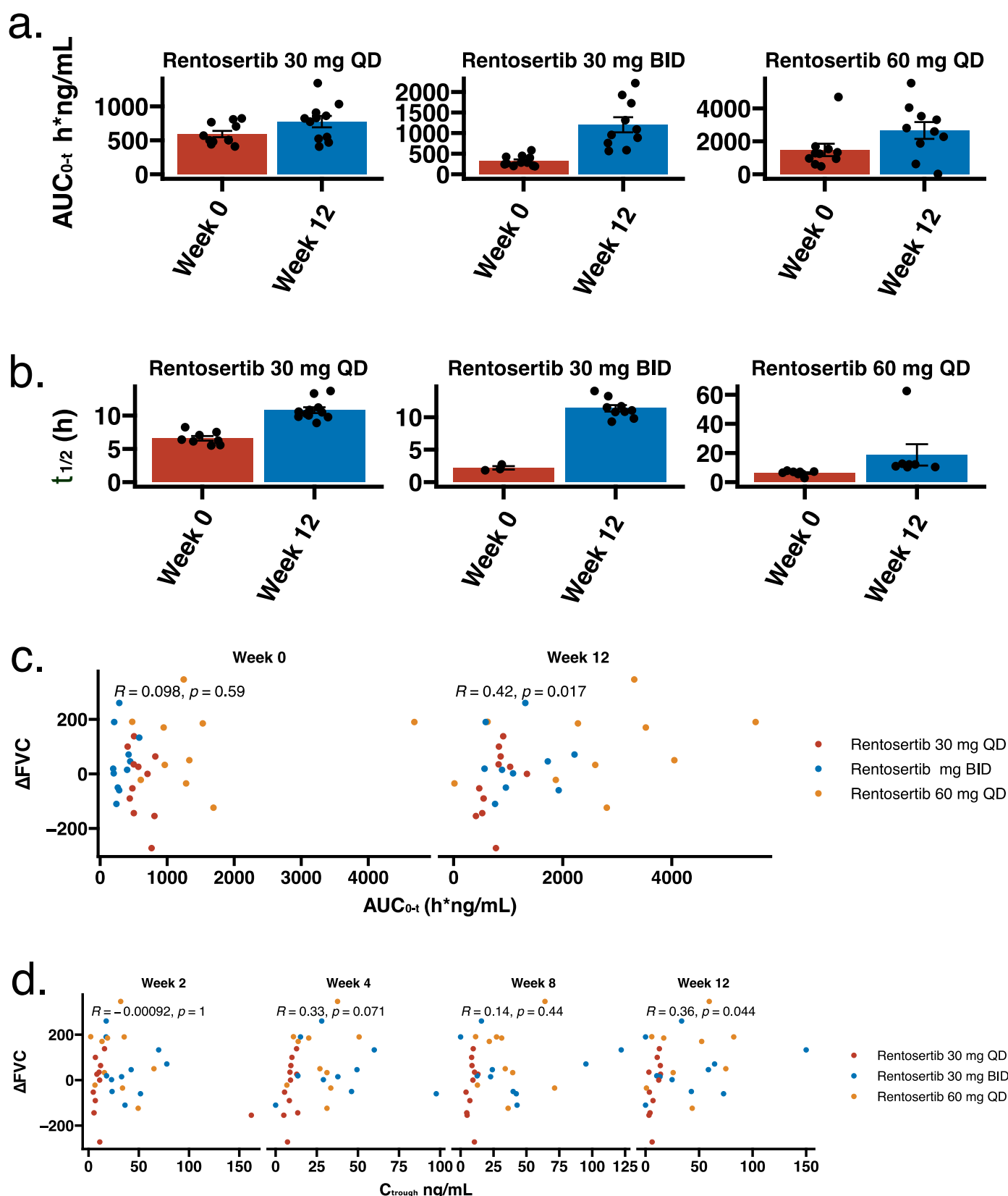ly taking antifibrotic therapy (right). (b) Absolute change in FVC ± 95% CI by ANCOVA Model with Multiple Imputation assuming missing at random (MAR) in patients not concurrently taking SOC antifibrotic therapy (left) or in patients concurrently taking antifibrotic therapy (right).
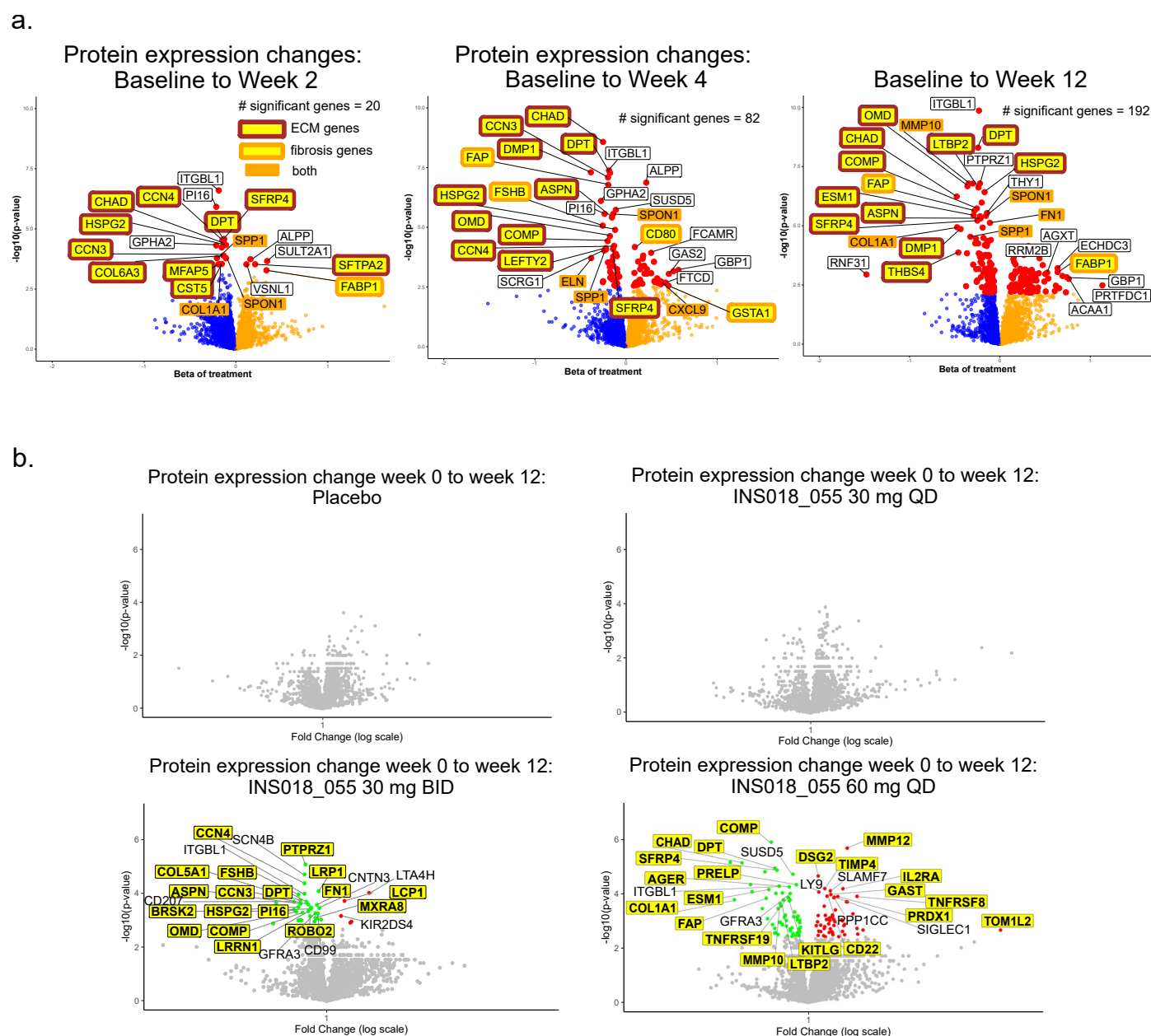
Extended Data Fig. 4 | Changes in additional lung function metrics after 12 weeks of treatment with rentosertib. (**a**) Absolute change in DLCO ± 95% CI. (**b**) Absolute Change in DLCO (% Predicted) ± SE, ANCOVA Model with Multiple Imputation assuming missing at random (MAR). (**c**) Absolute change in percent predicted HGB-corrected DLCO (%) ± SD. (**d**) Absolute change in FEV1 ± SD. (**e**) Mean percent-change in FEV1 ± SD. (**f**) Absolute change in LCQ score ± SD. (**g**) Absolute change in LCQ score ± SE by Mixed model for repeated measures (MMRM). (**h**) Absolute change in 6MWD ± SD. (**i**) Absolute change in 6MWD ± SE, ANCOVA Model with Multiple Imputation assuming MAR.
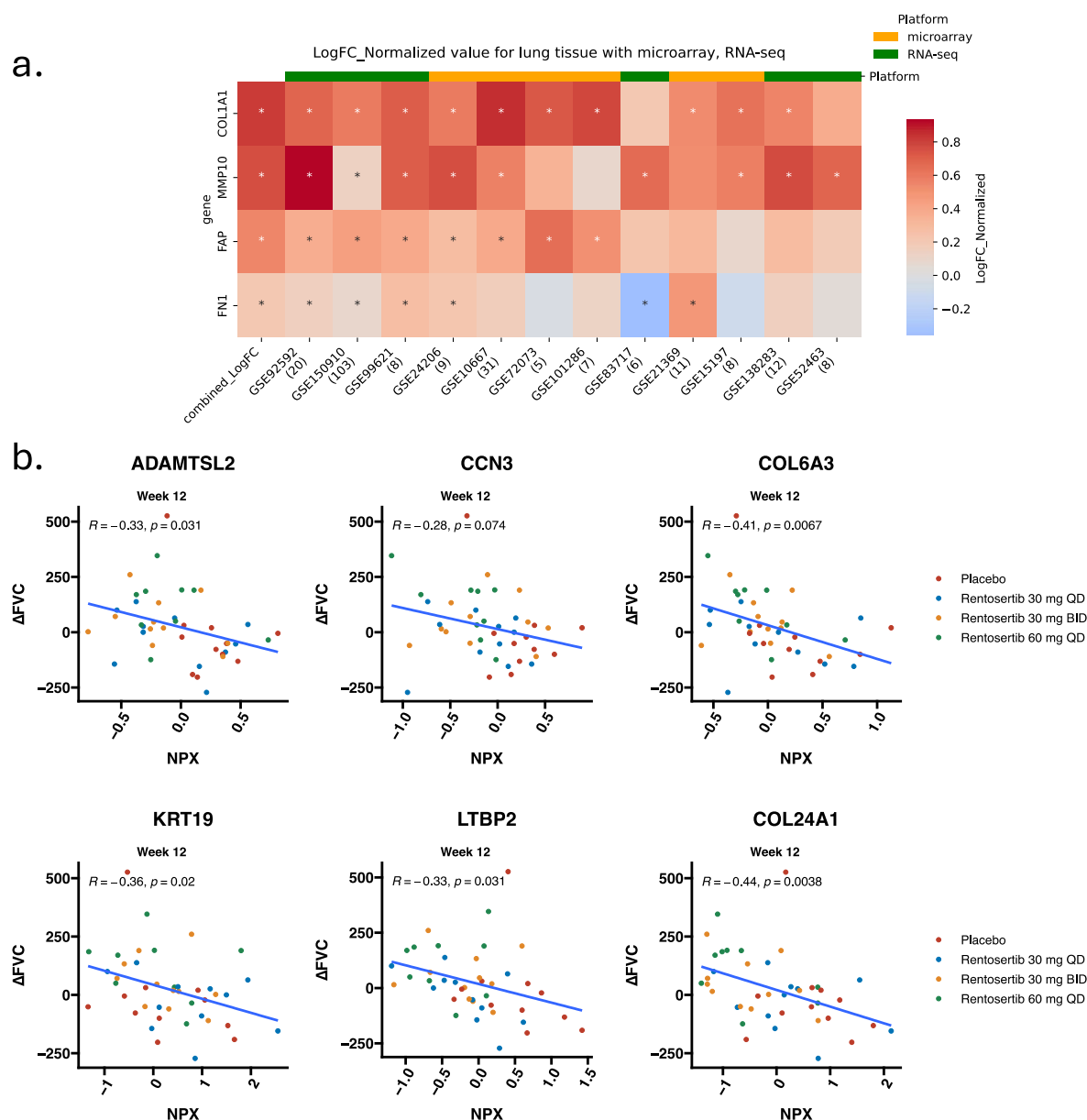
Extended Data Fig. 5 | Association of rentosertib treatment with PK parameters. (**a**) AUC$_{0-t}$ of rentosertib at week 0 and week 12, data are mean ± SD. n = 11 at week 0 and n = 11 at week 12 in 30QD, n = 11 at week 0 and n = 10 at week 12 in 30 BID, n = 10 at week 0 and n = 10 at week 10 in 60 QD. (**b**) t$_{1/2}$ of rentosertib at week 0 and week 12, data are mean ± SD. n = 11 at week 0 and n = 11 at week 12 in 30QD, n = 11 at week 0 and n = 10 at week 12 in 30 BID, n = 10 at week 0 and n = 10 at week 10 in 60 QD. (**c**) Correlation analysis of AUC$_{0-t}$ and change in FVC between week 0 and week 12. (**d**) Correlation analysis of C$_{trough}$ measured throughout the trial and change in FVC between week 0 and week 12. *P* values calculated by two-sided Spearman correlation analysis.

a.

b.

Extended Data Fig. 6 | Time- and dose-associated changes in serum protein expression associated with rentosertib treatment. (**a**) Change in Normalized Protein eXpression (NPX) from baseline to subsequent visits (weeks 4, 8, and 12) with a simple linear regression model (d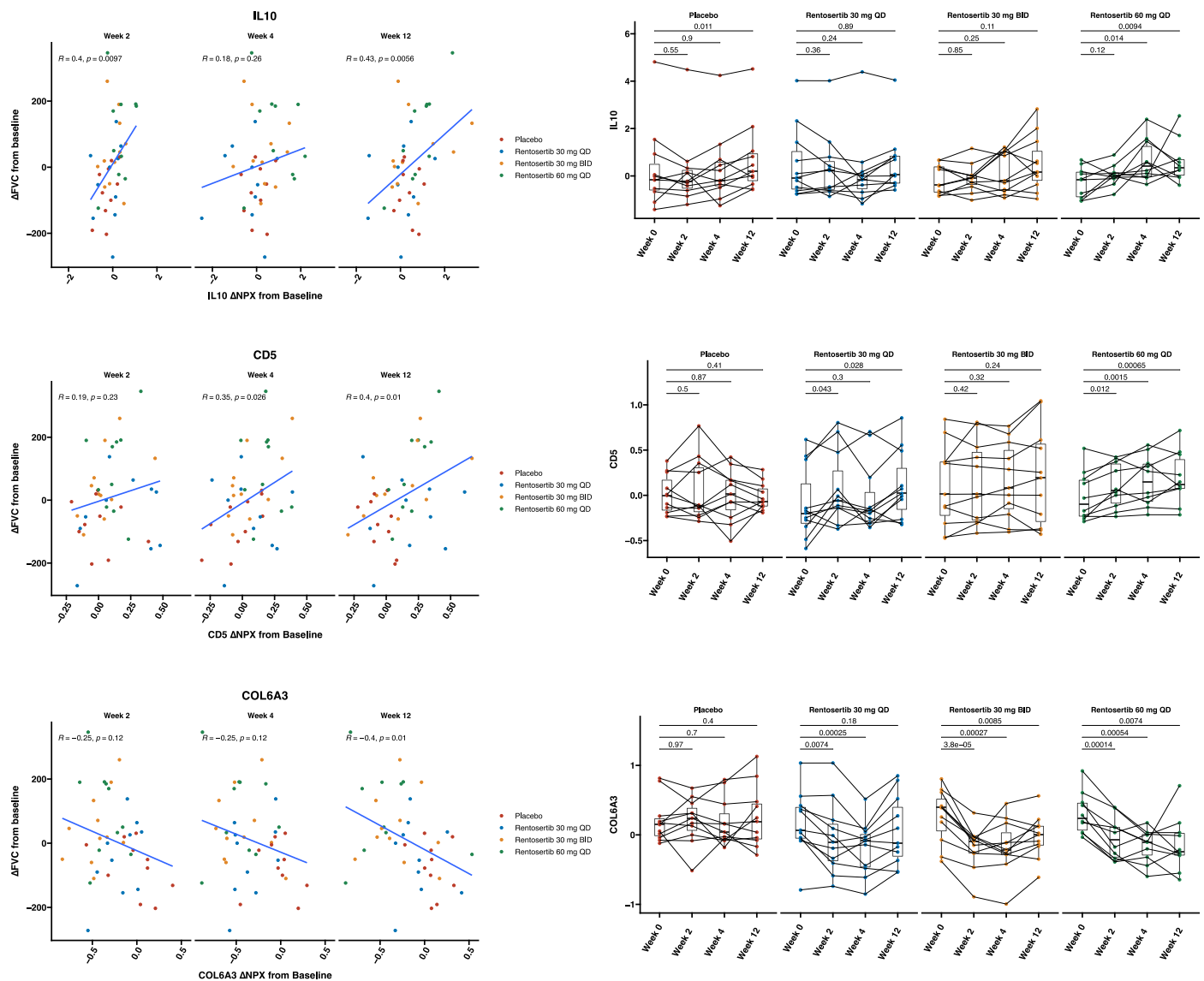elta_NPX ~ treatment_cat) fitted to assess the relationship between treatment dose and protein expression changes using Benjamini-Hochberg (BH)-adjusted *P* values. (**b**) Change in NPX between baseline and week 12 by two-sided paired BH-adjusted t-test. Red dots denote proteins with BH-adjusted *P* value < 0.1. Yellow boxes highlight fibrosis-related proteins.

Extended Data Fig. 7 | Serum proteins with changes in expression associated with changes in FVC with rentosertib treatment. (**a**) PandaOmics analysis of published RNA-seq gene expression datasets profiling patients with IPF and healthy individuals of four top proteomics hit genes in our trial cohort. (**b**) Correlation analysis of protein abundance of genes previously associated with lung function and IPF TFS with change in FVC from week 0 to week 12, treatment regimen, and time on treatment. n = 43 patient at each visit, and the *P* value was calculated by two-sided Pearson correlation analysis; n = 11 patients in Placebo, n = 11 patients in 30 QD; n = 11 patients in 30 BID, n = 10 patients in 60 QD. *P* values calculated by paired t-test.

Extended Data Fig. 8 | Correlation analysis of protein abundance of genes previously associated with aging-related dysfunction. Correlation analysis of protein abundance of genes (IL10, CD5, COL6A3) previously associated with aging-related dysfunction, such as immunity and ECM remodeling, with change in FVC from week 0 to week 12 and time on treatment. Left panel: n = 43 patient at each visit; *P* values calculated by two-sided Pearson correlation analysis; Right panel: n = 11 patients in placebo, n = 11 patients in 30 QD; n = 11 patients in 30 BID, n = 10 patients in 60 QD, boxes and whiskers are quartiles; *P* values calculated by paired t-test.

Corresponding author(s): Alex Zhavoronkov, Zuojun Xu

Last updated by author(s): Apr 2, 2025

Reporting Summary

Nature Portfolio wishes to improve the reproducibility of the work that we publish. This form provides structure for consistency and transparency in reporting. For further information on Nature Portfolio policies, see our Editorial Policies and the Editorial Policy Checklist.

Statistics

For all statistical analyses, confirm that the following items are present in the figure legend, table legend, main text, or Methods section.

n/a	Confirmed	
☐	☒	The exact sample size (*n*) for each experimental group/condition, given as a discrete number and unit of measurement
☒	☐	A statement on whether measurements were taken from distinct samples or whether the same sample was measured repeatedly
☐	☒	The statistical test(s) used AND whether they are one- or two-sided *Only common tests should be described solely by name; describe more complex techniques in the Methods section.*
☐	☒	A description of all covariates tested
☐	☒	A description of any assumptions or corrections, such as tests of normality and adjustment for multiple comparisons
☐	☒	A full description of the statistical parameters including central tendency (e.g. means) or other basic estimates (e.g. regression coefficient) AND variation (e.g. standard deviation) or associated estimates of uncertainty (e.g. confidence intervals)
☐	☒	For null hypothesis testing, the test statistic (e.g. *F*, *t*, *r*) with confidence intervals, effect sizes, degrees of freedom and *P* value noted *Give P values as exact values whenever suitable.*
☒	☐	For Bayesian analysis, information on the choice of priors and Markov chain Monte Carlo settings
☒	☐	For hierarchical and complex designs, identification of the appropriate level for tests and full reporting of outcomes
☒	☐	Estimates of effect sizes (e.g. Cohen's *d*, Pearson's *r*), indicating how they were calculated

Our web collection on statistics for biologists contains articles on many of the points above.

Software and code

Policy information about availability of computer code

Data collection	No software used to collect data.
Data analysis	Custom code to analyze proteomics data at https://codeocean.com/capsule/4095438/tree/v1.; PandaOmics (commercially available), R (v4.4.2), clusterProfiler R package (v4.13.4), lme4 R package (v1.1-35.5)

For manuscripts utilizing custom algorithms or software that are central to the research but not yet described in published literature, software must be made available to editors and reviewers. We strongly encourage code deposition in a community repository (e.g. GitHub). See the Nature Portfolio guidelines for submitting code & software for further information.

Data

Policy information about availability of data

All manuscripts must include a data availability statement. This statement should provide the following information, where applicable:

- Accession codes, unique identifiers, or web links for publicly available datasets
- A description of any restrictions on data availability
- For clinical datasets or third party data, please ensure that the statement adheres to our policy

Complete de-identified Olink proteomics data, demographics, and FVC data is deposited at the OMIX database at https://ngdc.cncb.ac.cn/omix/release/ OMIX008341.

Research involving human participants, their data, or biological material

Policy information about studies with [human participants or human data](). See also policy information about [sex, gender (identity/presentation), and sexual orientation]() and [race, ethnicity and racism]().

Reporting on sex and gender	Study cohort consisted of self-reported males and females, as listed in Table 1. Any bias in sex composition is reflective of incidence of IPF in the population. No sex- or gender-based analyses are reported.
Reporting on race, ethnicity, or other socially relevant groupings	The study participants are all of self-reported Asian race due to the study being conducted exclusively in China. This is listed in Table 1.
Population characteristics	Trial participants were all previously diagnosed with IPF as a criteria for inclusion. Patients were not excluded or included based on prior SOC antifibrotic therapy administration, but any concomitant antifibrotic use must have been stable for >8 weeks prior to screening. Patient mean age 66.7 (min 52, max 81, SD 6.7). Patient population was 90.1% male. Mean BMI 25.36 (min 16.3, max 33.9, SD 3.4).
Recruitment	Patients were recruited to the trial by site investigators. Prior to patient participation in the study, written informed consent was otained from each patient (or the patient's legally accepted representative) according to ICH-GCP standards and to the regulatory and legal requirements of the participating country. The investigator or delegate gave a full explanation to study patients based on the patient information form. A language understandable to the patient was chosen, technical terms and expressions avoided, if possible. Translation was provided where needed. The patient was given sufficient time to consider participation in the study. No self-selection or other bias was expected.
Ethics oversight	Each participating study institution was required to get approval from their Institutional Review Board (IRB / Independent Ethics Committee (IEC and competent authority (CA) according to national and international regulations.

Note that full information on the approval of the study protocol must also be provided in the manuscript.

Field-specific reporting

Please select the one below that is the best fit for your research. If you are not sure, read the appropriate sections before making your selection.

☒ Life sciences ☐ Behavioural & social sciences ☐ Ecological, evolutionary & environmental sciences

For a reference copy of the document with all sections, see [nature.com/documents/nr-reporting-summary-flat.pdf]()

Life sciences study design

All studies must disclose on these points even when the disclosure is negative.

Sample size	A target of 15 subjects was assigned to each treatment arm. . Approximately 70 patients will be enrolled to ensure approximately 60 patients complete treatment of 12 weeks. Given an approximate sample size of 15 subjects per treatment arm, there exists a 90% probability of observing at least 1 AE if the true population rate is approximately 15%, which is sufficient to assess the feasibility of safety parameters, the primary study objective.
Data exclusions	No data was excluded. One efficacy (FVC) analysis excluded n=1 patient from the placebo group and n=1 patient from the ISM001-055 30 mg QD group who exhibited >600 mL difference between screening and baseline FVC measurements, making uncertain the baseline FVC values in those patients. This is made clear in the Extended Data figure in which the analysis is shown.
Replication	Not applicable to phase 2a clinical trial data. Exploratory proteomics analyses not repeated due to limited biological material and cohort size.
Randomization	Patients were randomized 1:1:1:1 to each treatment arm.
Blinding	Subjects, investigators, site study staff, reviewers, and everyone involved in study conduct or analysis, were blinded with regard to the randomized treatment assignments until after data freeze. Bioanalytics staff were allowed to identify samples from subjects assigned to placebo treatment but did not disclose randomization until trial unblinding.

Reporting for specific materials, systems and methods

We require information from authors about some types of materials, experimental systems and methods used in many studies. Here, indicate whether each material, system or method listed is relevant to your study. If you are not sure if a list item applies to your research, read the appropriate section before selecting a response.

Materials & experimental systems

n/a	Involved in the study
☒ ☐	Antibodies
☒ ☐	Eukaryotic cell lines
☒ ☐	Palaeontology and archaeology
☒ ☐	Animals and other organisms
☐ ☒	Clinical data
☒ ☐	Dual use research of concern
☒ ☐	Plants

Methods

n/a	Involved in the study
☒ ☐	ChIP-seq
☒ ☐	Flow cytometry
☒ ☐	MRI-based neuroimaging

Clinical data

Policy information about clinical studies

All manuscripts should comply with the ICMJE guidelines for publication of clinical research and a completed CONSORT checklist must be included with all submissions.

Clinical trial registration

NCT05938920

Study protocol

Study protocol will be made available with publication.

Data collection

The trial was conducted at 21 sites across China beginning July 19, 2023, and running through June 11, 2024.
Participating study sites:
Anhui Chest Hospital, Hefei, Anhui, China, 230031
The Second Affiliated Hospital of Anhui Medical University, Hefei, Anhui, China, 230601
Peking University Shougang Hospital, Beijing, Beijing, China, 100041
Beijing Friendship Hospital, Capital Medical University, Beijing, Beijing, China, 100050
Peking Union Medical College Hospital, Chinese Academy of Medical Sciences, Beijing, Beijing, China, 100730
The First Affiliated Hospital, Sun Yat-sen University, Guangzhou, Guangdong, China, 510080
Nanfang Hospital of Southern Medical University, Guangzhou, Guangdong, China, 510515
Hainan General Hoapital, Haikou, Hainan, China, 570311
The First Affiliated Hospital of Zhengzhou University, Zhengzhou, Henan, China, 450052
Xiangya Hospital of Central South University, Changsha, Hunan, China, 410008
The Second Xiangya Hospital of Central South University, Changsha, Hunan, China, 410011
Nanjing Drum Tower Hospital, Nanjing, Jiangsu, China, 210008
Jiangxi Provincial People's Hospital, Nanchang, Jiangxi, China, 330006
The Shengjing Hospital of China medical university, Shenyang, Liaoning, China, 110004
Qilu Hospital of Shandong University, Jinan, Shandong, China, 250013
Shanghai Chest Hospital, Shanghai, Shanghai, China, 200030
Zhongshan hospital Fudan University, Shanghai, Shanghai, China, 200032
Shanghai Pulmonary Hospital, Shanghai, Shanghai, China, 201800
Shanxi Bethune Hospital, Taiyuan, Shanxi, China, 030032
The West China Hospital of Sichuan University, Chengdu, Sichuan, China, 610041
General Hospital of Tianjin Medical University, Tianjin, Tianjin, China, 300052
The First Affiliated Hospital - Zhejiang University School of Medicine, Hangzhou, Zhejiang, China, 310006

Outcomes

The primary objective of this study was to evaluate the safety and tolerability of orally administered ISM001-055 for up to 12 weeks in adult patients with IPF compared to placebo. The primary end point for this study was the percentage of patients who have at least 1 treatment-emergent adverse event (TEAE). Patients were continually monitored for AEs during the 12 weeks of rentosertib treatment and for one week following administration of the final dose, with study drug-related SAE and AESI collected if they occurred beyond the study period. Medical judgement of the site investigators was used to determine whether there was a reasonable possibility of a causal relationship between an AE and the given study treatment.

The secondary efficacy endpoints measured the relative and percent change in FVC from week 0/visit 2 up to week 12. The absolute and relative change in FVC % predicted from week 0/visit 2 up to week 12 was also measured. The change in DLCO % predicted from week 0/visit up to week 12 and, the change in Leicester Cough Questionnaire (LCQ) from week 0 to weeks 4, 8, and 12 were also analyzed. The change in 6-minute walk distance (6MWD) in meters from week 0 to week 12 was also evaluated. FVC and FEV1 measured at baseline/randomization with centrally sourced SpiroSphere devices (Clario) provided by the sponsor with study-specific training and proficiency tests to the operating staff to meet the 2019 ATS/ERS guideline criteria with central overread. DLCO measurements were all assessed with devices from each site according to the ATS/ERS guidelines, and all measurements were conducted with the same equipment for each site.

Other secondary end points included pharmacokinetic parameters of ISM001-055 and related metabolites following the first dose at visit 2 and the last dose at visit 6 (EOT) from blood samples drawn at weeks 0, 2, 4, 8, and 12. This study also collected data on the number of acute IPF exacerbations and the number of days hospitalized following acute IPF exacerbations from week 0 through week 12.

The Leicester Cough Questionnaire (LCQ) is a 19-item questionnaire that assesses cough related QOL taken at weeks 0, 4, 8, and 12.

The exploratory end points analyzed include the change in IPF blood biomarkers following ISM001-055 treatment at weeks 0, 2, 4, 8,

and 12. Changes in the blood proteome in treated patients were also measured at these time points.

Plants

Seed stocks

Report on the source of all seed stocks or other plant material used. If applicable, state the seed stock centre and catalogue number. If plant specimens were collected from the field, describe the collection location, date and sampling procedures.

Novel plant genotypes

Describe the methods by which all novel plant genotypes were produced. This includes those generated by transgenic approaches, gene editing, chemical/radiation-based mutagenesis and hybridization. For transgenic lines, describe the transformation method, the number of independent lines analyzed and the generation upon which experiments were performed. For gene-edited lines, describe the editor used, the endogenous sequence targeted for editing, the targeting guide RNA sequence (if applicable) and how the editor was applied.

Authentication

Describe any authentication procedures for each seed stock used or novel genotype generated. Describe any experiments used to assess the effect of a mutation and, where applicable, how potential secondary effects (e.g. second site T-DNA insertions, mosiacism, off-target gene editing) were examined.